THE JOURNAL OF COMPARATIVE NEUROLOGY 429:22–44 (2001)

Structure of Longitudinal Brain Zones That Provide the Origin for the Substantia Nigra and Ventral Tegmental Area in Human Embryos, as Revealed by Cytoarchitecture and Tyrosine Hydroxylase, Calretinin, Calbindin, and GABA Immunoreactions

CATHERINE VERNEY,[1]* NADA ZECEVIC,[2] AND LUIS PUELLES[3]
[1]INSERM U.106, Hôpital Salpêtrière, 75651 Paris Cedex 13, France
[2]University of Connecticut Medical School, Farmington, Connecticut 06030
[3]Department of Morphological Sciences, University of Murcia, Murcia E30100, Spain

ABSTRACT

In a previous work, mapping early tyrosine hydroxylase (TH) expressing primordia in human embryos, the tegmental origin of the substantia nigra (SN) and ventral tegmental area (VTA) was located across several neuromeric domains: prosomeres 1–3, midbrain, and isthmus (Puelles and Verney, [1998] J. Comp. Neurol. 394:283–308). The present study examines in detail the architecture of the neural wall along this tegmental continuum in 6–7 week human embryos, to better define the development of the SN and VTA. TH-immunoreactive (TH-IR) structures were mapped relative to longitudinal subdivisions (floor plate, basal plate, alar plate), as well as to radially superposed strata of the neural wall (periventricular, intermediate, and superficial strata). These morphologic entities were delineated at each relevant segmental level by using Nissl-stained sections and immunocytochemical mapping of calbindin, calretinin, and GABA in adjacent sagittal or frontal sections. A numerous and varied neuronal population originates in the floor plate area, and some of its derivatives become related through lateral tangential migration with other neuronal populations born in distinct medial and lateral portions of the basal plate and in a transition zone at the border with the alar plate. Some structural differences characterize each segmental domain within this common schema. The TH-IR neuroblasts arise predominantly within the ventricular zone of the floor plate and, more sparsely, within the adjacent medial part of the basal plate. They first migrate radially from the ventricular zone to the pia and then apparently move laterally and slightly rostralward, crossing the superficial stratum of the basal plate. Several GABA-IR cell populations are present in this region. One of them, which might represent the anlage of the SN pars reticulata, is generated in the lateral part of the basal plate. J. Comp. Neurol. 429:22–44, 2001.

Indexing terms: catecholamines; segmentation; prosomeres; calcium-binding proteins; floor plate; basal plate

We reported recently a neuromeric and topologic mapping of the characteristic positions occupied by catecholaminergic, tyrosine hydroxylase-immunoreactive (TH-IR) neurons in the brain of early human embryos (4–6 gestation weeks; Puelles and Verney, 1998). Among other aspects, we corroborated a previous suggestion that several of the catecholaminergic primordia of vertebrates

Grant sponsor: INSERM, ECC; Grant number: CI1 CT90 0848; Grant sponsor: CICYT; Grant number: PB98 0397.

*Correspondence to: Catherine Verney, INSERM E9935, Hôpital Robert Debré; 48, Bd Sérurier, 75019 Paris, France. E-mail: cverney@infobiogen.fr

Received 20 April 2000; Revised 28 July 2000; Accepted 28 July 2000

are plurisegmental in origin (see Puelles and Medina, 1994). The substantia nigra (SN) and the ventral tegmental area (VTA) are two examples; they originate in a continuum extending across the isthmus, midbrain, and the three diencephalic prosomeres (p1–p3; Puelles and Rubenstein, 1993; Puelles 1995). The relevant ventral areas of these prosomeres jointly constitute the classic prerubral tegmentum, intercalated between the mammillary pouch and the nucleus ruber and oculomotor nerve complex in the midbrain tegmentum.

Conventional anatomical description assigns this entire tegmental domain to the midbrain (Kuhlenbeck 1973; but see Gilbert 1935; Keyser 1972; Nieuwenhuys 1998). This follows an early tentative definition of the mesdiencephalic limit by His (1890), who "provisionally" set this boundary as an arbitrary line connecting the posterior commissure, dorsally, with the mammillary region, ventrally. This early view was soon superseded technically by Palmgren's (1921) well-documented definition of the midbrain-diencephalic boundary: this passes behind the posterior commissure and in front of the magnocellular nucleus ruber in all vertebrates. This embryologic conception has been corroborated by modern molecular markers (Puelles and Rubenstein, 1993; Puelles, 1995), i.e., confirmed by the caudal expression boundary of the gene *Pax-6* at the mes-diencephalic boundary (Stoykova and Gruss, 1994; Schubert et al., 1995), whereas there is no marker support for His' (1893) tentative limit. The use of His' limit by the Nomina Anatomica led to the view that structures occupying the retromamillary and prerubral tegmental region belong to the midbrain; this is the case of the rostral parts of the TH-IR SN and VTA (Puelles and Medina, 1994; Puelles and Verney, 1998). The approach followed in this study is consistent with Palmgren's (1921) embryologic concept of the midbrain, and, therefore, describes the main dopaminergic formations—SN and VTA (A9 and A10; Dahlström and Fuxe, 1964)—as a large continuum of TH-IR-positive cells extending from the isthmus into the diencephalon (is, mes, p1–p3), as recently mapped in detail in sagittally sectioned human embryos (Puelles and Verney, 1998).

A clearer understanding of the multiple origin, migration, and initial histogenesis of the SN and VTA formations requires data on the cytoarchitecture of the whole tegmental region at the midbrain-diencephalon transition. This structure can be best characterized in cross-sections transversal to the brain axis. We particularly need more precise data on the longitudinal neuronal columns originating at the floor, basal, and alar plates in this area, as well as on any additional internal structural subdivisions which might be detected within these main longitudinal zones. There may also exist different strata (radial subdivisions), or longitudinal subdivisions of the longitudinal columns, as suggested by Palmgren (1921) and Rendahl (1924). Parallel observations on collocalization of TH with calbindin in human embryos (Verney et al., 1992; see also a companion paper, Verney et al., 2000), as well as the example of multiple marker approach provided by the mouse developmental atlas of Jacobowitz and Abbott (1998), suggested to us that the calcium-binding proteins calbindin D28K (CaBP) and calretinin (CalR) would be useful as markers for floor plate (FP) and basal plate (BP) subdivisions in the human midbrain and caudal forebrain. Mapping of GABA-immunoreactive cell populations was attempted as well, to describe the development of the SN pars reticulata, whose adult phenotype is GABA-ergic (Oertel et al., 1982), and whose precise origin remains unknown.

To understand the structural organization of this region, sagittal and transverse sections stained alternatively with different markers were examined. The major technical difficulty of such a study is that strict transverse sections cannot always be made, due to the sharp axial bend of the cephalic flexure; the section plane of any cross-section series consequently varies across the flexure, e.g., changing from a frontal to an oblique, or even horizontal, plane. Allowing for this, the use of calcium-binding proteins as differential markers of neuronal differentia-

Abbreviations

III	oculomotor nucleus and nerve
IIIv	third ventricle
IV	trochlear nucleus and nerve
AP	alar plate
APtz	alar plate transitional zone
aq	aqueduct
B	nucleus of Bechterew
BP	basal plate
BPm	medial basal plate
BPl	lateral basal plate
cb	cerebellar primordium
CP	commissural pretectum
DT	dorsal thalamus
dtc	deep tegmental commissure
eg	epichordal central group
EMT	eminentia thalami
es	epichordal strip
ET	epithalamus
ew	nucleus of Edinger-Wesphal
FP	floor plate
fr	fasciculus retroflexus
ims	intermediate migratory stream
if	isthmic fovea
is	isthmus
iz	intermediate zone or stratum
ma	mammillary area
mr	mammillary recess
mes	mesencephalon
mfb	medial forebrain bundle/nigrotelencephalic tract
mlf	medial longitudinal fasciculus
mms	marginal migratory system
mtg	mammillotegmental tract
nmlf	nucleus of the medial longitudinal fasciculus
npc	nucleus of the posterior commissure
p1–p4	prosomeres names in Figs. 1, 2
pc	posterior commissure
pm	paramedial group
PP	precommissural pretectum
pv	periventricular zone or stratum
ri	rostral intertitial nucleus
rn	red nucleus
SC	superior colliculus
SN	substantia nigra
sr	subrarubral nucleus
st	subthalamic nucleus
stc	superficial tegmental commissure
sz	superficial or marginal zone (stratum)
VT	ventral thalamus
vz	ventricular zone
zl:	zona limitans intrathalamica

TABLE 1. Human Embryos Included in the Present Study

Gestation weeks[1]	Carnegie stage	Plane of section	Specimen[2]
6 (17)	18	Frontal	N19 (0/8)
6.5 (20)	20	Frontal	N18 (0/8)
7 (26)	22	Sagittal	N26 (0/8)

[1]Gestation weeks were in fact postovulatory weeks. Numbers in parentheses indicate the crown-rump length in millimeters.
[2]Numbers in parentheses indicate postmortem delay/fixation time in hours.

tion, associated to Nissl staining in adjacent sections, nevertheless revealed a great deal of the structural detail of the ventral longitudinal zones within the relevant neuromeres.

MATERIAL AND METHODS

The three human embryos studied in this work lacked neuropathologic alterations and were obtained from legal abortions (Table 1). The protocol used received the approval of the French National Ethics Committee (CCNESVS) (Zecevic and Verney, 1995). The embryos and fetuses were staged according to the Carnegie stages (Müller and O'Rahilly, 1994). The whole embryos were fixed in 4% paraformaldehyde in phosphate buffer (pH 7.4, 0.12 M) for 8 hours, rinsed and cryoprotected in phosphate buffer added with 10% sucrose, and cut in serial cryostat sections (12 μm). Groups of adjacent sections were rinsed in phosphate-buffered saline containing 0.25% Triton X and 0.2% gelatin (PBS-gel-TX) and incubated in primary antisera for 24 to 72 hours. Antibodies were diluted in PBS-gel-TX containing 10% human serum albumin (Sigma): monoclonal anti-TH antibody (Incstar, Stillwater, MN; 1:1,000); polyclonal anti-TH antiserum raised in rabbits (Vigny and Henry, 1981, 1:6,000); polyclonal anti-CaBP and anti-calretinin antisera raised in rabbits (Swant, Bellinzona, Switzerland; 1:20,000); monoclonal anti-GABA antibody (Sigma, Saint Louis, MO; 1:3,000). The labeling was visualized using the streptavidin-biotin-peroxydase method (Amersham, Little Chalfon, UK) with DAB as chromogen, as described previously by Verney et al. (1993). After four 15-minute washes, sections were incubated with biotinylated anti-rabbit or -mouse IgG (1/200) (2 hours) and rinsed (2 × 10 minutes) in PBS-gel-TX. Incubation in streptavidin-biotin-peroxidase complex (1/400 in PBS-gel-TX) (2 hours) was followed by two washes (10 minutes in PBS) before the revelation of peroxidase in H_2O_2 (0.002%) and 3,3′-diaminobenzidine tetrahydrochloride (0.05%), 10 to 20 minutes. After two washes in distilled water, the sections were dehydrated in graded series of alcohol, and mounted in Permount. Controls where the primary antibody was omitted were made to check the absence of cross-reactivity with the secondary antibodies. Contiguous adjacent sections were stained with thionine for cytoarchitectonic analysis.

For each segmental domain, we examined the respective longitudinal zones, as defined cyto- and chemoarchitectonically, and the periventricular, intermediate, and eventual superficial strata of each sector were analysed. The putative primordia of known nuclei or fiber tracts were identified, and unnamed cell populations were assigned tentative positional names. The large size of the human brain helps the identification of cyto- or chemoarchitectonic entities that might otherwise remain unnoticed in the brain of smaller species (e.g., rodents). Subsequently, we proceeded to map more accurately the topology of TH-positive dopaminergic and GABA-positive neurons of the SN and the VTA.

RESULTS

Results will be presented in three sections. First, an overview of the transverse and longitudinal subdivisions at the midbrain-diencephalon boundary neighborhood is provided, as identified in sagittal and transverse sections by means of specific anatomical landmarks and the major calcium-binding protein immunoreaction patterns. Then, we describe in more detail the structure and immunochemical staining pattern of the floor plate (FP), basal plate (BP), and the ventralmost part of the alar plate (AP) region, where it bounds upon the BP across a distinct region that was provisionally called by us the "alar transition zone" (APtz). Finally, the resulting detailed morphologic framework is contrasted with the distribution maps of TH- and GABA-immunoreactive neurons.

Overview of longitudinal/transversal subdivisions and relevant landmarks

Figure 1 shows representative sagittal sections of embryo N26 (stage 22), stained with four of the markers used in this study (thionine, CaBP, CalR, TH). An overview of the region examined is schematized in Figure 2. Figures 3–9 correspond to embryo N18 (stage 20); these panels show successive rostrocaudal cross-sections, whose respective rostrocaudal levels, and varying topology with regard to the curved length axis, are shown in Figure 2. Drawings of frontal sections at four significant levels show the different prosomeres and the longitudinal floor plate (FP), basal plate (BP), alar transitional zone (APtz), and alar plate (AP) (Fig. 3). Some of these planes are fairly transverse to the tegmentum at the cephalic flexure, resulting in true cross-sections of the diencephalic prosomeres p2 (Figs. 3B, 5, 6) and p1 (Figs. 3C, 7, 8). Conversely, other section levels are oblique or horizontal relative to the retromammillary and mammillary areas in p3 and p4, respectively (ma; Figs. 2, 3A, 4) or to the midbrain tegmentum and the isthmo-mesencephalic boundary (mes, is; Figs. 2, 3D, 9).

The following anatomic landmarks were used to locate the relevant transverse interneuromeric boundaries: isthmic fovea and trochlear decussation (isth/mes limit just in front of them), posterior commissure (mes/p1 limit just behind it), fasciculus retroflexus (p1/p2 limit just behind it), zona limitans intrathalamica (coinciding with the p2/p3 limit), and an external notch limiting caudally the mammillary pouch (coinciding with the p3/p4 limit) (Figs. 1A, B, 2). A series of alar plate regions, thus, can be delimited: the superior colliculus (mes), the pretectum (p1), the dorsal thalamus and epithalamus (p2), and the ventral thalamus (p3). Each overlies a tegmental (basal/floor) sector, whose structure may reveal common aspects, as, e.g., the origin of the ventral tegmental area and substantia nigra dopaminergic populations (Fig. 1D; see also Puelles and Verney, 1998), or distinctive features, as the oculomotor nucleus in the midbrain, the nucleus of the posterior commissure in p1, or the subthalamic nucleus in p4 (III; npc; st; Fig. 2).

Calretinin has a distinct pattern of expression in the tegmental region extending from the isthmus to the mam-

millary pouch. It shows limited expression at the floor plate (see below), and is virtually absent in the alar plate cell populations. However, it is strongly expressed throughout a tegmental periventricular area, which may represent the basal plate radial domain, because it includes the area occupied by the oculomotor nucleus in the midbrain (see CalR-immunostained sections, all labeled D, in Figs. 4–9). This basal CalR expression domain is also observed in sagittal sections (framed by dash lines in Fig. 1C). CaBP is expressed in cells close to the floor plate midline (see below) and in some cell groups found within the basal plate, although only in the p3, p2, and mes basal plate, as defined by CalR (CaBP in Figs. 4–6, 9). Sections through the p1 basal plate are devoid of these CaBP-IR elements, except for the CaBP-IR neurons of the npc (compare CalR and CaBP in Figs. 7, 8, see below). After comparing our immunohistochemical material with the thionin-stained sections, in which the main longitudinal boundaries are suggested by differences in the relative thickness of the ventricular zone, we have postulated that the boundaries between floor plate and basal plate, on one hand, and alar and basal plates, on the other, indeed may correspond to the sharp medial and lateral limits of CalR expression in the tegmentum, respectively. Calbindin immunoreaction serves as an accessory, although less useful, marker of these longitudinal columns, because this marker labels many fibers, and is widely distributed in the alar plate. Curiously, sections through p2 selectively show a small stripe of ependymal CaBP-IR cells, placed precisely at the locus identified above as the alar-basal boundary. This finding suggests the existence of a longitudinal palisade of CaBP-IR radial glia cells along this longitudinal limit within the p2 prosomere (see Discussion section).

The diencephalic and mesencephalic alar plates typically contain many CaBP-positive fibers and/or cells, and the corresponding ventricular and mantle layers are heavily populated (Fig. 1A, B; Nissl and CaBP sections A, C in Figs. 4–9). A longitudinal transitional zone, which usually contains fewer CaBP-IR fibers in p1 and midbrain levels, and whose ventricular and periventricular strata are less thick, separates the alar-basal boundary from the well-developed alar plate mantle (thionin sections A- in Figs. 3–8). We have provisionally called this intercalated longitudinal subregion the alar plate transition zone (APtz; Fig. 1A, B; Figs. 3–9). This zone merits distinction because it displays specific histogenetic and chemoarchitectonic features, which are described below. Nevertheless, structurally it seems more akin to the alar plate than to the basal plate.

The floor plate domain common to the midbrain and the three diencephalic prosomeres is characterized by a particularly dense cytoarchitecture (described in more detail below), as well as by the inverted-fountain pattern of TH-IR cells and fibers of the ventral tegmental area and

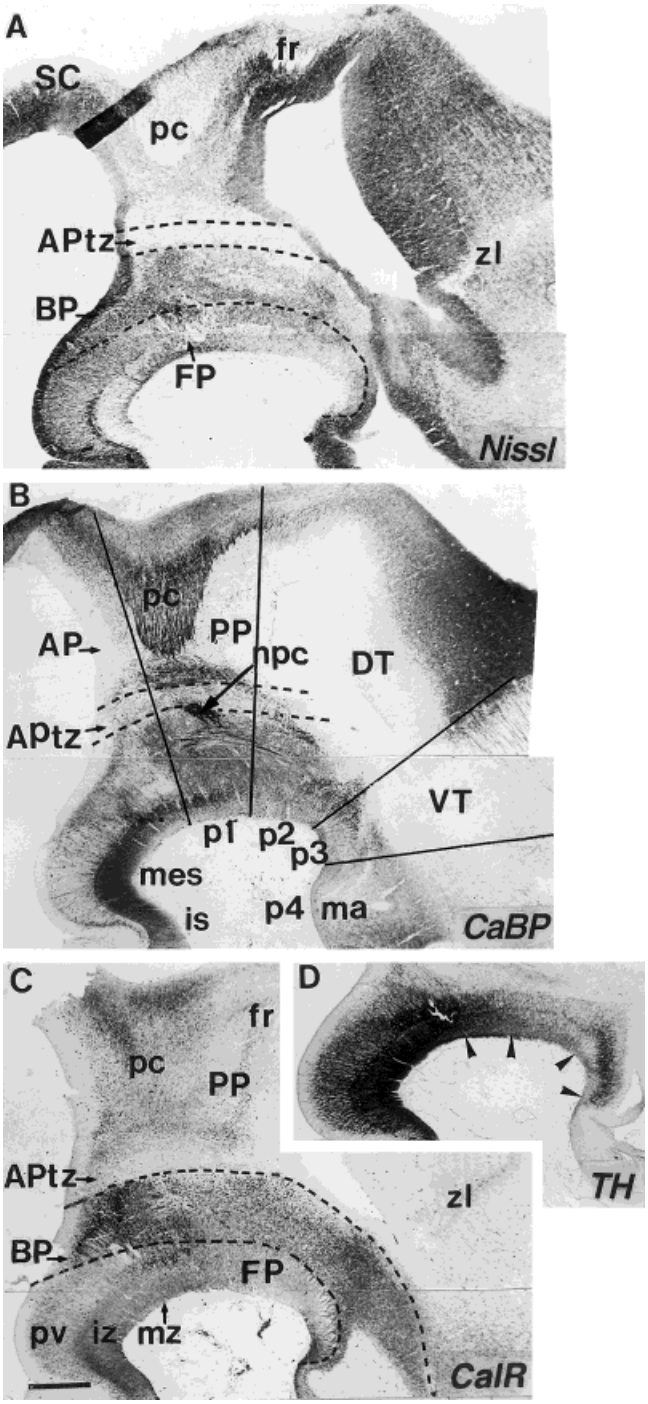

Fig. 1. Adjacent parasagittal sections of case N26 stained with thionin (**A**), calbindin D28K (CaBP; **B**), calretinin (CalR; **C**), and tyrosine hydroxylase (TH; **D**) immunoreactivity, respectively. The Nissl-stained section (A) shows some anatomical landmarks (pc, posterior commissure; fr, fasciculus retroflexus; zl, zona limitans), which identify the transverse interneuromeric boundaries delimiting the diverse segments studied, i.e., mes, p1, p2, p3, as shown with black lines in B. The posterior commissure (pc) and its basal nucleus (npc) and the dorsal thalamus (DT) are strongly CaBP immunoreactive (B). Dotted lines delimit the floor plate (FP) from the basal plate (BP) in A and C, and the alar plate transition zone (APtz) from the BP and alar plate (AP). The basal plate (BP) appears globally CalR immunoreactive, with a clear-cut basal/alar boundary (C), strung from the mesencephalon to the mammillary pouch (mes, p1-p4, ma in B). Tyrosine hydroxylase immunoreactivity is restricted to FP and BP (D). Note the different patterns of cell distribution observed in the different prosomeres (limits indicated by arrowheads). mz, marginal zone. For other abbreviations, see list. Scale bar = 200 μm in C (applies to A–D).

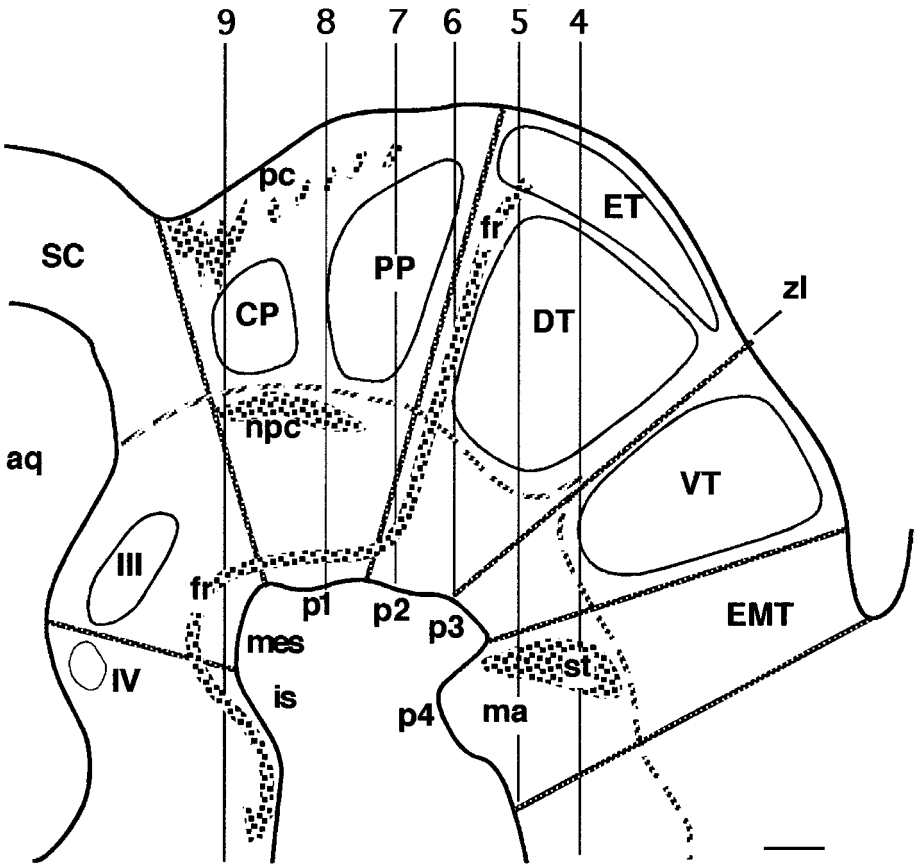

Fig. 2. Schematic drawing of the different structures, landmarks, and boundaries observed at a sagittal level similar to that shown in Figure 1. The transverse neuromeric boundaries from isthmus (is) to p4 are drawn as straight lines, and the limit between the basal and alar plate is represented by the curved dash-dotted line, parallel to the cephalic flexure. The planes of coronal sections shown in Figures 4–9 are indicated by vertical lines. For abbreviations, see list. Scale bar = 200 μm.

SN (FP; VTA; Figs. 4–9). The sharp lateral cytoarchitectonic limit of the floor plate coincides with the boundary delineated by CalR immunostaining in the adjacent basal plate (jointly with CaBP immunoreaction in mes, p2, and p3). Both CalR and CaBP also appear in distinct cell populations developing at or near the midline of the floorplate (named 'epicordal strip' by Puelles et al., 1987); similar positive neurons characteristically seem to disperse superficially and lateralward through the inverted fountainhead zone (Figs. 4–9).

Detailed organization of FP, BP, and transitional AP

For description purposes, we will consider the tegmental neural wall divided into a ventricular zone and periventricular, intermediate, and marginal strata of the mantle zone. At stage 20, the FP, BP, and AP zones are delimited in Nissl material by changes in the thickness of the ventricular zone, which is distinctly thicker in the AP and thinnest in the BP (Figs. 3–8). A cell-poor gap separates the ventricular and periventricular zones in the FP, BP, and APtz, but is absent in the rest of the AP (Figs. 4–6).

The floor plate: cytoarchitecture

The floor plate displays a similar structure across mes, p1, p2, and p3 (Fig. 3); this is best described in transverse sections (our Figs. 4–8; compare levels in Fig. 2). Within the floor plate, we distinguish a median epichordal strip and a bilateral paramedian region. In Nissl-stained material, the median plane consists of a thin strip of ependymoglial cells, whose pial processes are arranged in a median radial palisade; the mantle layer here is relatively cell-poor but varies from one locus to another (see below). This formation corresponds to the epichordal strip entity first described in the chick (Puelles et al., 1987), and resembles somewhat the epichordal, vimentin-positive radial glial palisade present at the midline of the hindbrain raphe (Kingsbury, 1920; Vaage, 1969; Kuhlenbeck, 1973; Puelles, 1995, and unpublished observations), although its cells are shorter radially. Lateral to the epichordal strip appear the heavily populated paramedian floorplate regions. These are divided into a dense (more basophilic) periventricular zone and a less dense (paler) intermediate zone (pv; iz; Figs. 6A–8A); crossing fibers form a deep tegmental commissure between these two cellular strata (dtc; Figs. 7A–C, 8A–C). The subpial marginal zone at the

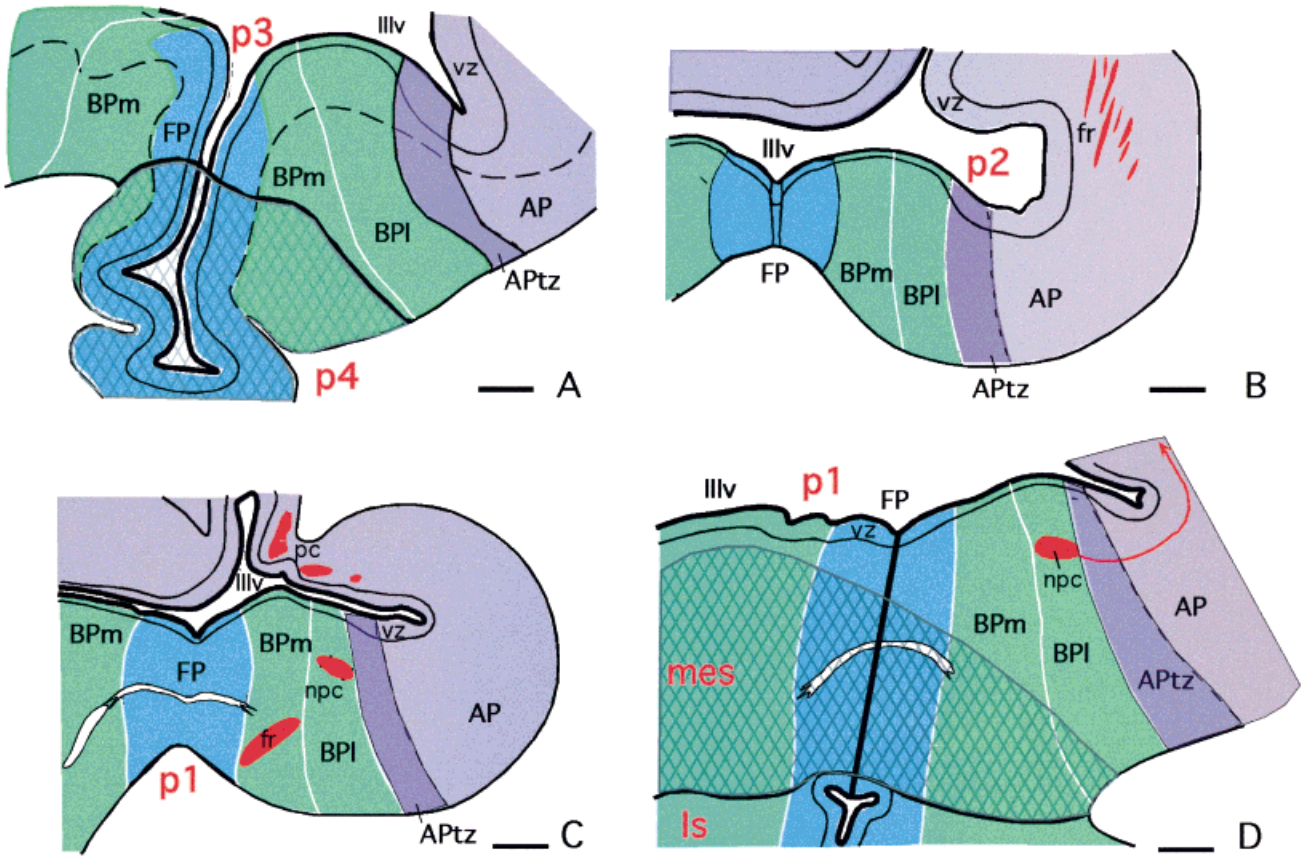

Fig. 3. Schematic drawings of the longitudinal subdivisions recognized in frontal sections selected at the level of p3-p4 (**A**), p2 (**B**), p1 (**C**), and p1-mesencephalon-isthmus (**D**). The prosomere p4 and the mesencephalon are hatched. The floor plate (FP) territory is in blue, the medial and lateral basal plate (BPm, BPl) in green, the alar plate transitional zone (APtz) in dark purple, and the alar plate (AP) in purple. Anatomic landmarks serving to locate the neuromeric limits are in red, like the fasciculus retroflexus (fr) close to the p1/p2 limit, or the nucleus of the posterior commissure (npc) and posterior commissure (pc), at the p1-mesencephalic boundary. For other abbreviations, see list. Scale bars = 200 μm in A–D.

surface of the FP is thinly populated by neurons and contains mainly fibers (mz; Figs. 6A–8A), some of which intercross in a superficial tegmental commissure (this is best detected at caudal midbrain levels, due to the crossing of CaBP-IR/CalR-IR fiber bundles; stc; Fig. 9B–D). The paramedian floorplate region also can be subdivided into a medial domain (adjacent to the epichordal strip) rich in cells immunoreactive for CaBP and CalR and a lateral domain poor in such cells, although these domains are not strictly delimited. At section levels through p1 (and less clearly in mes), a number of periventricular cells apparently invade the epichordal strip and accumulate in a sizeable central mass at the interface of the periventricular and intermediate strata (Fig. 7A); this central cell group stains distinctly with the CaBP and CalR antibodies (compare Fig. 7C,D and see below).

The floor plate: CalR and CaBP immunoreactivity

The ventricular zone of the floor plate region is uniformly negative for these markers from mes to p3. Labelling in the mantle subzones will be described separately for the p2–p3 and p1-midbrain sectors.

A. In p2 and p3, the FP periventricular zone shows a subset of radially oriented, pale-staining CaBP-IR neurons and cell processes, which concentrate and show higher immunoreactivity particularly within the medial half of the paramedian floorplate region, adjacent to the negative epichordal strip (Figs. 5C, 6C). The subajacent intermediate zone contains widely dispersed strongly positive CaBP-IR cells. Their positions and perikaryal orientation suggests these cells may be migrating obliquely laterally and obliquely into the adjoining BP marginal zone (Figs. 5C, 6C). The associated deep tegmental commissure contains fibers moderately immunoreactive for CaBP at these levels.

CalR-IR neurons are also found in the periventricular zone of the paramedian FP but not in the epichordal strip; they are strongly immunoreactive and are rather sparse (there are even fewer in the lateral part of the FPpz). These cells are often oriented obliquely, pointing either toward the epichordal strip or toward the lateral part of the deep tegmental commissure (Figs. 5D, 6D). A signifi-

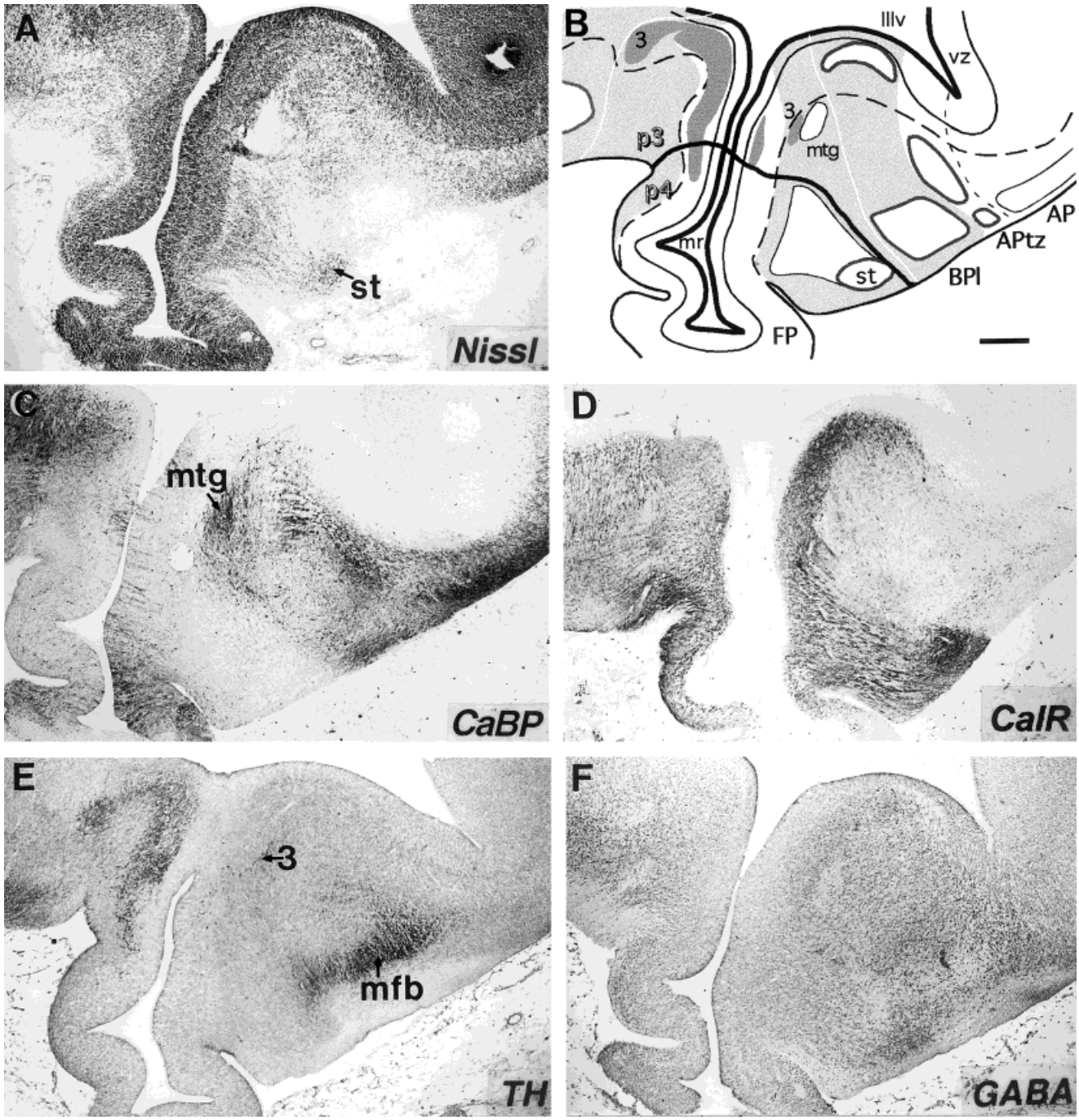

Figs. 4–9. Figures 4–9 display at one section level (indicated in Fig. 2) six panels from adjacent coronal sections of case N18 at stage 20, stained with thionin (**A**), next to a drawing with our structural interpretation (**B**), and sections illustrating calbindin D28K (CaBP; **C**), calretinin (CalR; **D**) tyrosine hydroxylase (TH, **E**) and γ-aminobutyric acid (GABA; **F**) immunoreactivity, respectively. The plane of sectioning is slightly asymmetric: the left half of each figure is more caudal than the right half. On the B panels are schematized the different neural domains delineated by cytoarchitecture and the different markers: long continuous lines along the ventricle delineate the ventricular zone (vz) and long-dash lines delimit the superficial border of the periventricular zone (pv). A short-dash line indicates at each level the limit between the alar plate transitional zone (APtz) and the alar plate (AP). The basal plate (BP) is shaded in light gray and the territory where TH immunoreaction is observed is shaded in darker gray. Dark gray outlines delineate the GABA-immunoreactive (IR) cell subpopulations within the BP and APtz. The locations of putative known nuclei or fiber tracts are indicated (see abbreviation list). Numbers show different subsets of TH-IR neurons; 1, TH-IR neurons in the marginal migratory system (mms); 2, TH-IR neurons in the intermediate migratory stream (ims); 3, subset of TH-IR neurons that originate in the BPm. Figs. 4, 5. **A–F:** As shown on the sagittal schema in Figure 2, these sections are in fact obliquely horizontal to p2, p3, and p4. The mammillary region in p4 is identified by the ventral mammillary recess (mr) and the migratory source of the subthalamic nucleus (st); note that the latter is calbindin D28K (CaBP) negative and calretinin (CalR) positive (C,D). Calretinin immunoreactivity in D delineates the BP, which is segregated into medial and lateral components (BPm and BPl; separated by a white line in B). For other abbreviations, see list. Scale bar = 200 μm in B (applies to A–F).

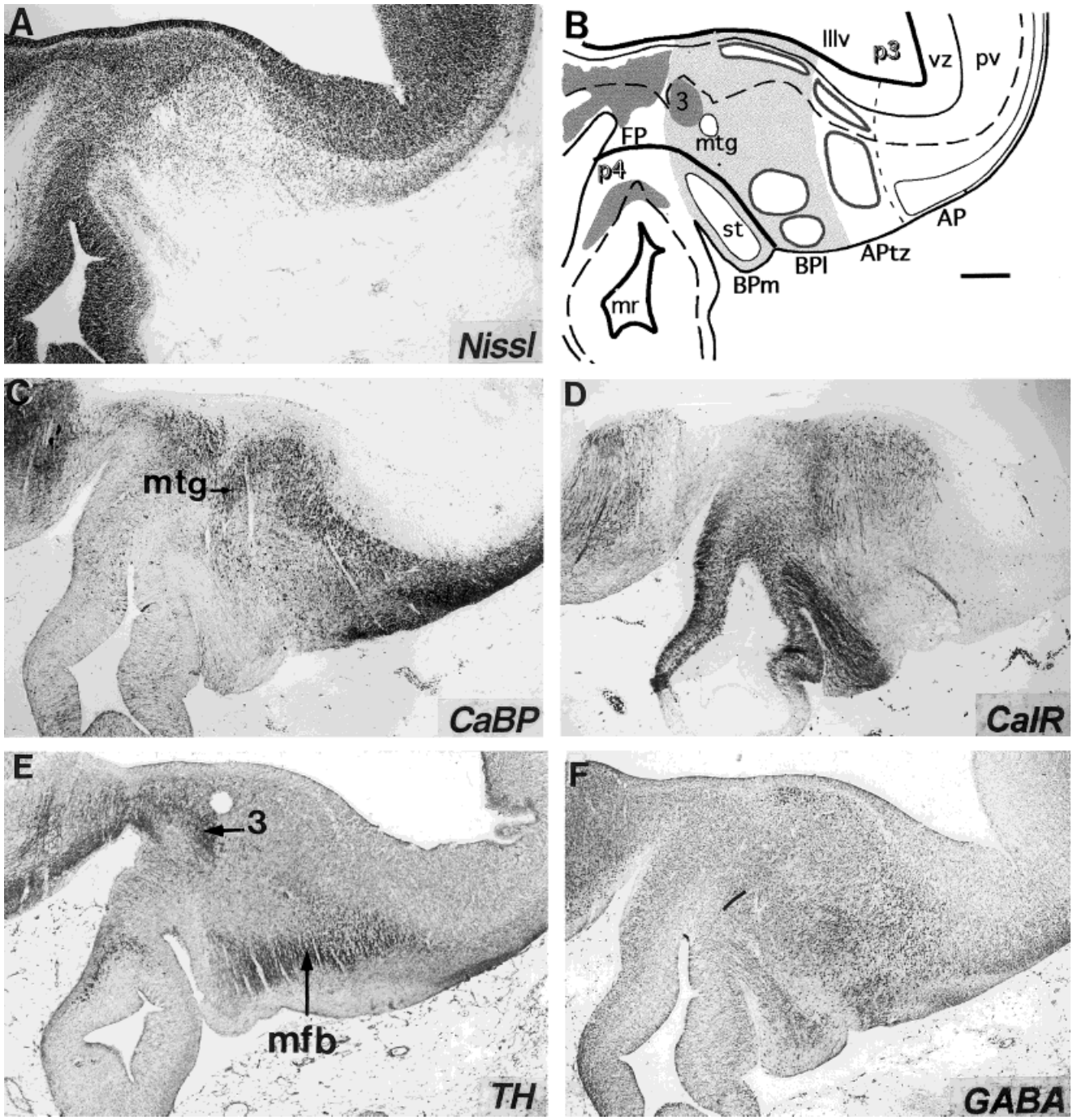

Fig. 5. See legend, Figure 4.

cant group of similar cells appears to stream out from the deep tegmental commissure into the intermediate zone of the BP, as suggested by the circumferential orientation of their leading processes (Figs. 5D, 6D). We called this group of cells the "intermediate migratory stream." In the intermediate zone of the FP, there are virtually no CalR-IR neurons at p2 and p3 levels, although a few cells, participating in a "marginal migratory stream" that enters the BP marginal zone, do express CalR (Figs. 5D, 6D).

B. In P1 and the midbrain, the overall CaBP and CalR floor plate expression pattern described in p2 and p3 is maintained, with the addition of a central group of CaBP/CalR-IR neurons, which aggregates at or around the epichordal strip, at the interface of the periventricular and intermediate zones (Figs. 7C,D, 8C,D, 9C,D, 10A,B). This central mass corresponds topographically to the anteromedian nucleus described in the literature (Leichnetz, 1982). A number of CaBP-IR neurons appear to leave the

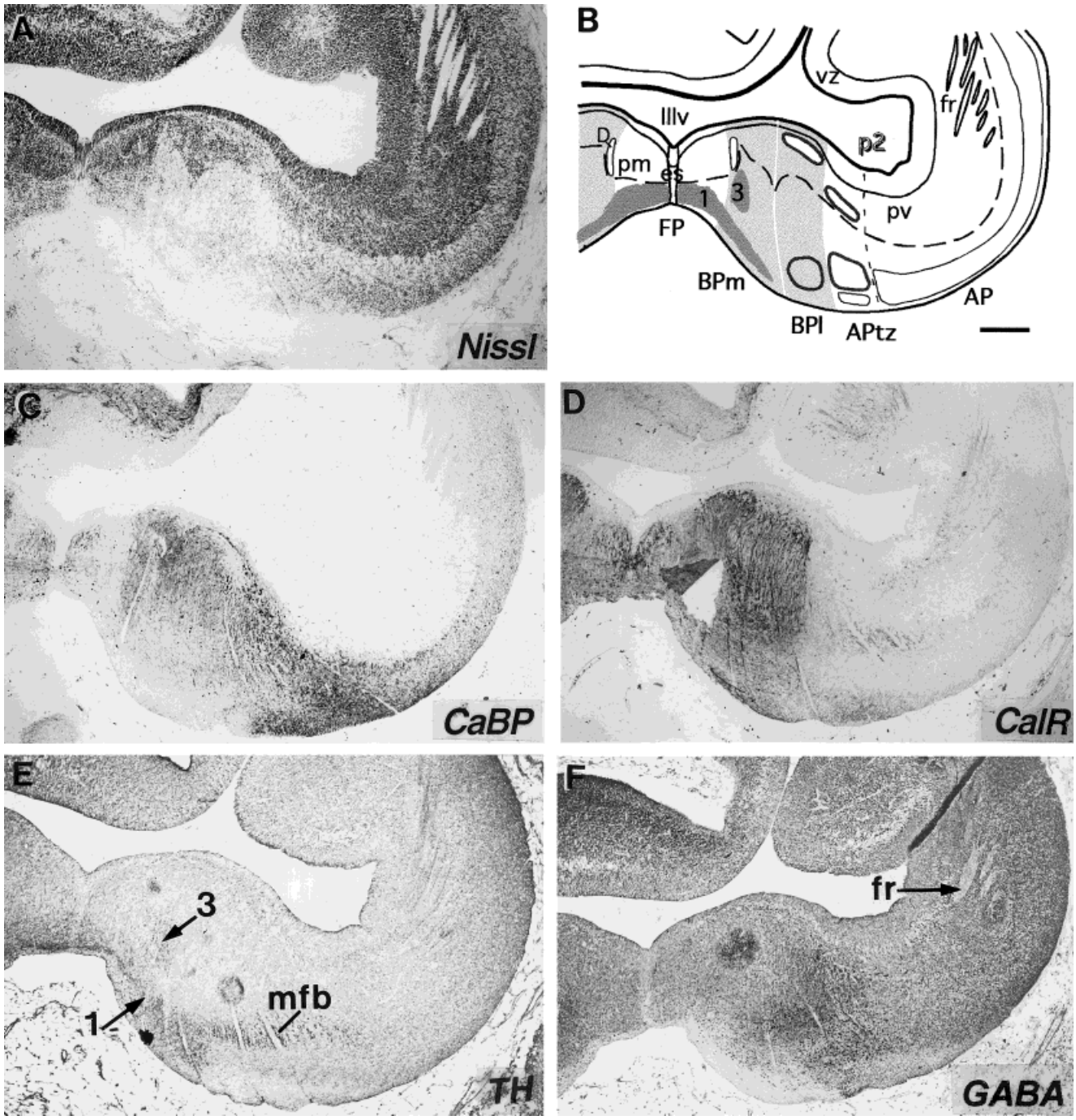

Figs. 6–8. **A–F:** As shown in Figure 2, these section levels are increasingly transverse, but pass still slightly obliquely through the p1/p2 boundary; the latter is marked by the strictly dorsoventral course of the fasciculus retroflexus (fr) in caudal p2. In Figure 6, the fr bends into its longitudinal course caudalward (check Fig. 2). The variations in cell density and thickness of the ventricular (vz) and periventricular zones (pv) observed in Nissl-stained material delineates clearly the longitudinal bands of the FP, medial and lateral BP, APtz, and AP. These boundaries are also outlined by the complementary pattern of calretinin (CalR) and calbindin D28K (CaBP) immunoreactivity. In p1, the nucleus of the posterior commissure (npc), which is CaBP immunoreactive (Figs. 7C, 8C) give rise to the pc fibers (unlabeled arrow in 7C, 8C). Arrowheads in Figures 7C,D, 8C,D indicate the epichordal central group. ru, rubral primordium. D, nucleus of Darkschewitsch. For other abbreviations, see list.

FP laterally and pass into the BP intermediate zone, following the intermediate migratory stream (ims in Figs. 7B, 8B, 10A,B), which begins at the level of the deep tegmental commissure. This cell stream only contained CalR-IR cells more rostrally, in p2 and p3. CaBP-IR neurons also seem to pass from the central or anteromedian

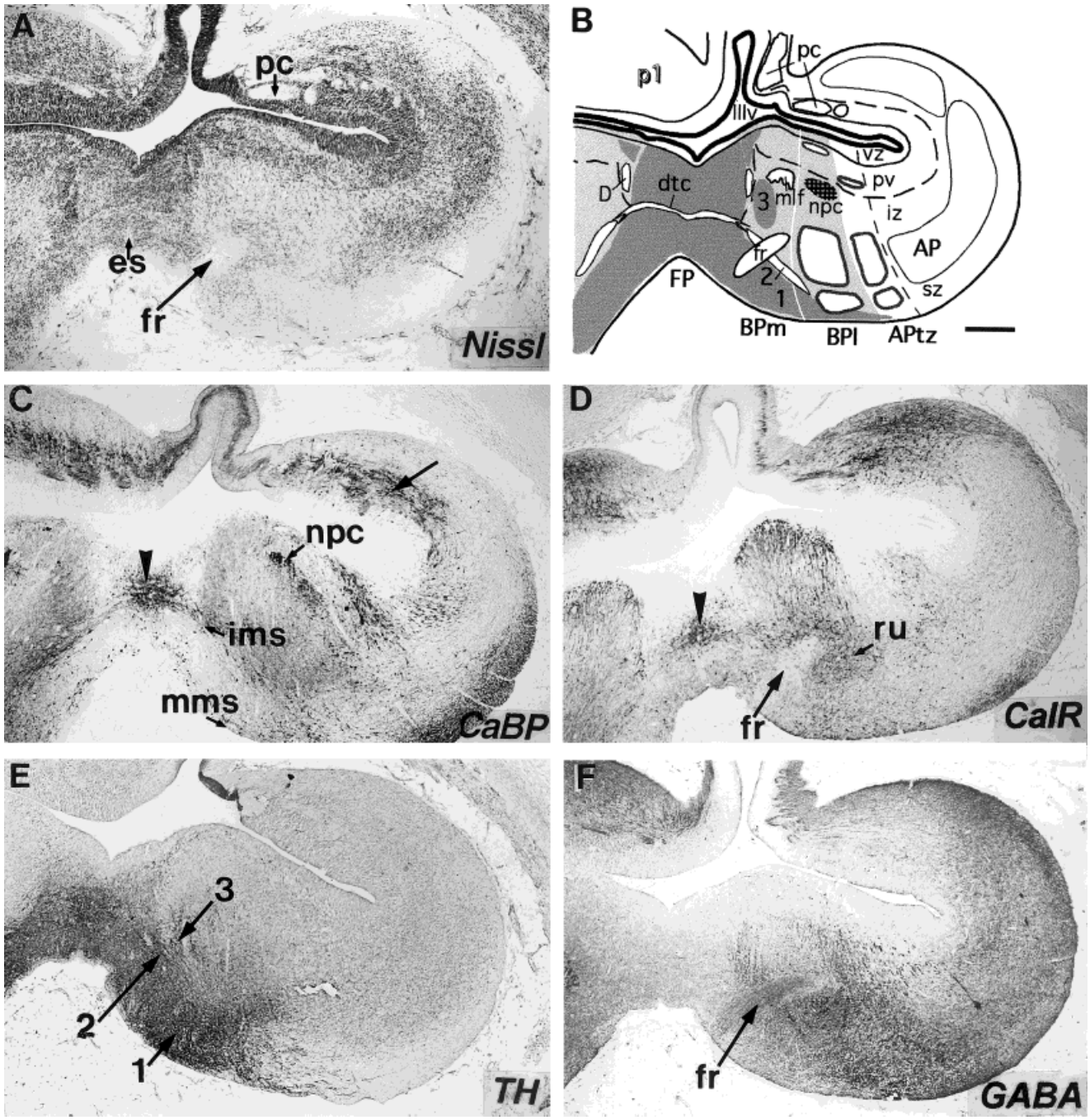

Fig. 7. See legend, Figure 6. For introductory comments, see legend, Figure 4.

mass bilaterally into the FP intermediate and marginal zones, and proceed laterally and forming what we have called the "marginal migratory stream" (mms), which enters laterally the BP marginal zone (Figs. 7B,C, 8B,C, 10A,B).

Basal plate: Cytoarchitecture

As mentioned above, the ventricular zone of the BP is much thinner than that of the AP and slightly thinner than that of the FP (Figs. 5A–8A). This difference is probably due to precocious differentiation of the BP, compared with AP and FP (His, 1904; Keyser, 1972; Puelles et al., 1987), resulting in earlier exhaustion of the BP neuroepithelium. The BP ventricular zone appears separated from the corresponding periventricular zone by a cell-poor gap, possibly also as a result of the end of neurogenetic activity. The wall domain identified in this way coincides neatly with that demarcated by CalR immunoreaction

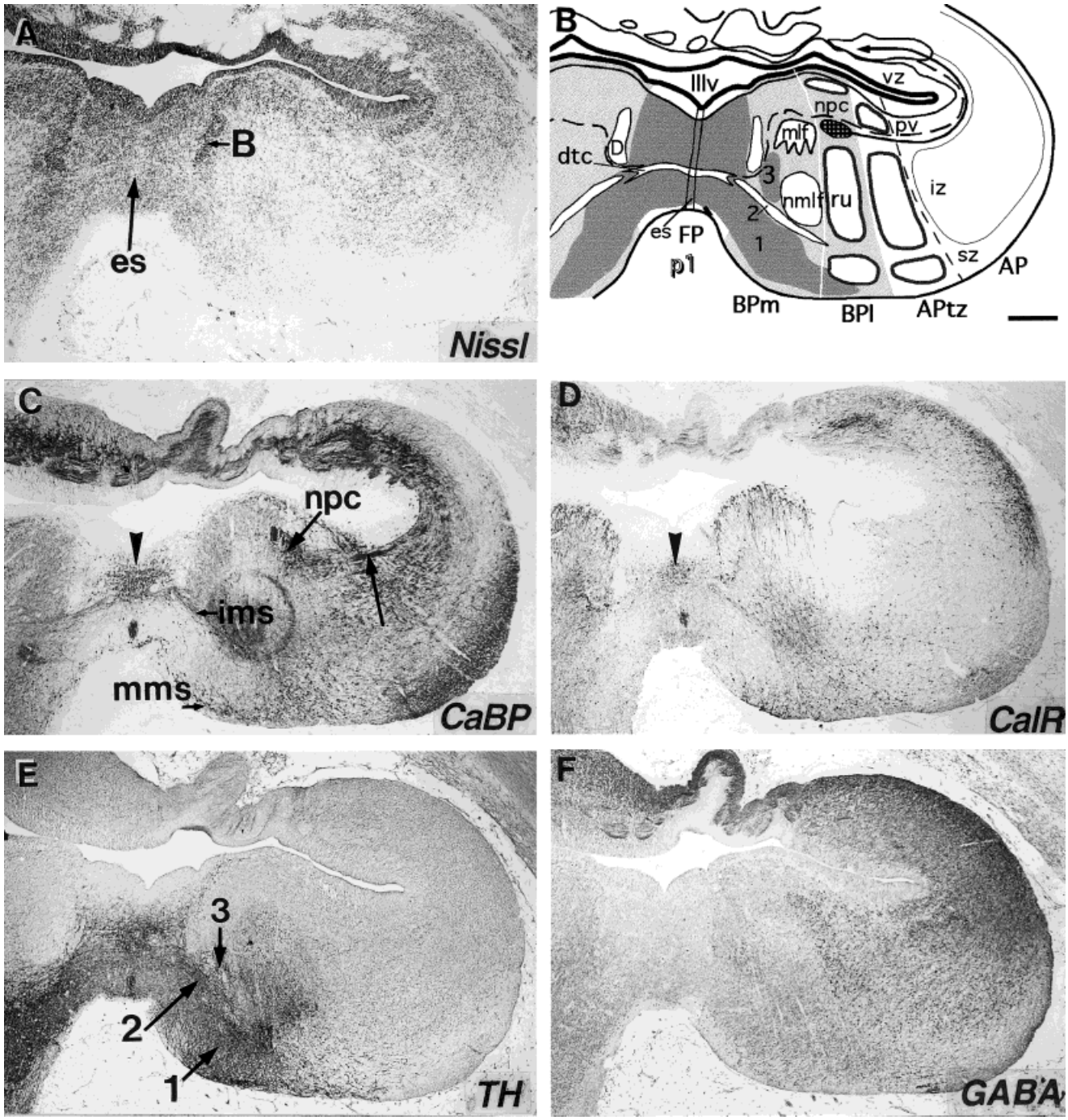

Fig. 8. See legend, Figure 6. For introductory comments, see legend, Figure 4.

(and CaBP immunoreaction in mes, p2, and p3), as is illustrated in Figures 4–10.

The CalR and CaBP markers also emphasize a longitudinal subdivision of the whole BP into medial and lateral parts, which are visualized in cross-sections as two ventrally concave arches of positive periventricular neurons (BPm, BPl in Figs. 4–9). Compared with the BPl, the arched BPm periventricular zone is slightly thicker, lies closer to the ventricular zone, and its cell population is denser. A particularly dense, dorsoventrally elongated neuronal aggregate found in the BPm, just adjacent to the FP, may correspond to the nucleus of Bechterew mentioned in the literature (B; Figs. 6A,B–8A,B), whereas less basophilic neurons found more laterally in the BPm may constitute the nucleus of Darkschewitsch (Leichnetz, 1982; Leichnetz et al.,

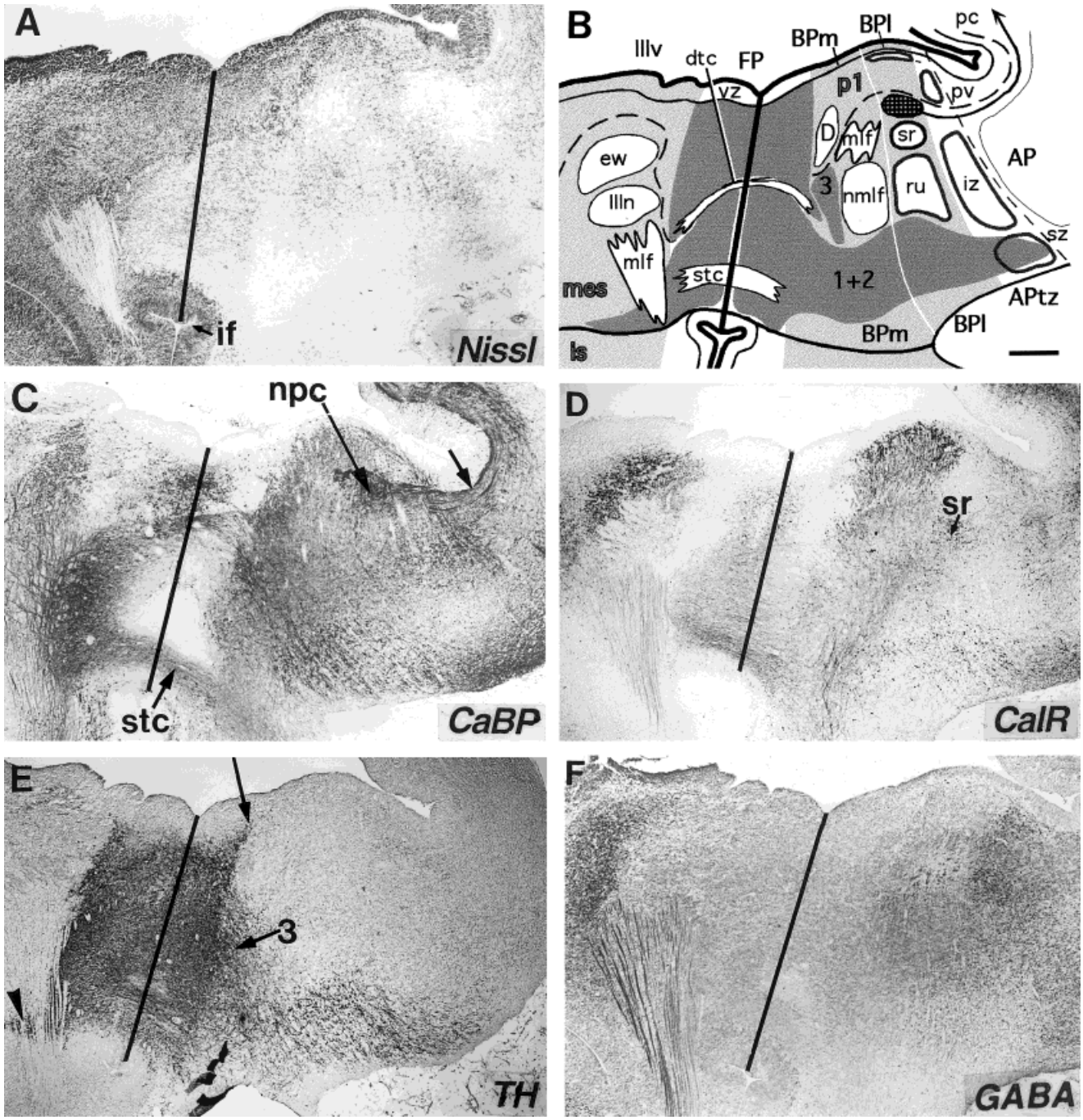

Fig. 9. **A–F:** As indicated in Figure 2, this section level corresponds to a horizontal section through the midbrain and isthmus: the left-right asymmetry of the sections is most marked at this level, so that midbrain and isthmus are sectioned at left side (note the oculomotor nucleus complex and nerve) and p1 at right. Arrowhead, the "deep migratory stream" at the isthmic level. We marked the FP midline with a black straight line in each panel, to help interpretations. The darkly hatched nucleus in B, which is calbindin D28K immunoreactive (Fig. 9C) is the nucleus of the posterior commissure giving rise to the pc fibers (curved arrow in B). D, nucleus of Darkschewitsch. For other abbreviations, see list.

1984). The subajacent BPm intermediate zone is dispersed by the passage of numerous longitudinal fiber bundles and does not allow definition of specific cell groups in Nissl-stained material. The BPm is crossed longitudinally by the CaBP-immunoreactive mammillotegmental tract and associated mammillopetal tracts and also, more caudally in p1 and mes, by the medial longitudinal tract (mtg; Figs. 4B,C, 5B,C; mlf; Figs. 8B, 9B). The BPm marginal zone is traversed mediolaterally by the marginal migratory stream originated in the FP.

The arched BPl periventricular zone appears subdivided into a relatively dense outer layer and a much less populated inner layer (e.g., see Figs. 6A, 7A). The corresponding intermediate zone is more extensive radially and has a reticular appearance. Nevertheless, at some section levels, there are densely aggregated cells deeply, near the periventricular zone (e.g., Figs. 4A, 5A); among these aggregates, the CaBP-immunoreactive, densely packed cells of the nucleus of the posterior commissure stand out in p1 (npc; panel C in Figs. 7–9). This intermediate stratum includes the deep tegmental area of the retromammillary area in p3, the rostral interstitial nucleus in p2, the interstitial nucleus of Cajal (nmlf nucleus), the nucleus of the posterior commissure (npc) in p1, and deep parts of the mesencephalic reticular formation in the midbrain. More dispersed cells found in the superficial half of the BPl intermediate zone of p1 may be the parvicellular part of the red nucleus (all descriptions in the literature agree that this nucleus is limited rostrally by the retroflex tract, the landmark for the p1/p2 boundary), whereas larger neurons occupying the same locus in the midbrain represent the magnocellular part of the red nucleus. Additional unidentified neuronal populations occupy this general area (superficial intermediate BPl zone) in p2 and p3, correlating with the vaguely defined posterior tuberculum and retromammillary areas (Puelles et al., 1987; Puelles, 1995). The marginal zone of the BPl also contains dispersed small neurons and apparently becomes invaded by tangentially migrating cells from the FP and BPm (see below).

Basal plate: CalR and CaBP immunoreactivity

Besides the variations of thickness and cell density of the ventricular and periventricular zones, which help to delimit and subdivide the BP, this column is characterized throughout by its CalR positivity. Strongly to moderately positive CalR-IR cell bodies are prevalent in the BP periventricular zone of p4 to mes, and they extend CalR-IR cell processes into the underlying intermediate stratum; these neurites, probably both dendrites and axons, are arranged radially as they enter the intermediate stratum underneath each of the BPm and BPl pv arches, creating the impression of a double constitution of the whole BP (Fig. 5D). These positive cell populations encompass the primordia of several mature nuclei, including the nucleus of Bechterew, nucleus of Darkschewitsch, and other periventricular entities sometimes subsumed under the concept of "ventral periacqueductal gray" (Figs. 4D–10D). The inner (deeper) sublayer of the BPl periventricular zone differs in that it only shows palely stained CalR-IR cells and a few CaBP-IR neurons; the latter typically tend to be disposed tangentially (panel C in Figs. 4–9), and coexist with a GABA-IR population (panels F in Figs. 4–9). Both CalR and CaBP seem to coexist in the BPm/BPl periventricular layer of p3, p2, and midbrain (Figs. 4–6, 9), but expression of CaBP largely disappears within the corresponding CalR-IR locus of p1 (Figs. 7, 8).

The distribution of CaBP in the intermediate zone of the BP is different in p3-p2 and p1. The p3 and p2 diencephalic prosomeres show an abundance of CaBP-IR fibers in the deep part of the intermediate zone and dispersed isolated positive neurons in the more superficial part (both BPm and BPl; Figs. 5, 6). In contrast, CaBP-IR fibers and cells largely disappear in the BP intermediate zone of p1, as in the local periventricular zone, with two remarkable exceptions. The deep BPl intermediate stratum in p1 shows an intensely CaBP-immunoreactive nucleus, whose positive efferent axons can be followed into the posterior commissure. This identifies it as the basal nucleus of the posterior commissure, a distinct primordium whose A/P position in p1 can be likewise associated in sagittal sections (npc; Fig. 1B, panels C in Figs. 7–10; note that other neuronal groups in the p1 alar plate also are associated to the posterior commissure). The second exception is the intermediate and marginal migratory streams of CaBP-IR cells, which spread out lateralward from the FP into the BP intermediate and marginal zones, respectively (ims, mms; Figs. 7, 8, 10).

Extensive CalR expression is found in the deep layer of the BP intermediate zone of p3, p2 (Figs. 4–6); In the BPl of caudal p1, CalR-IR cells form a rounded "suprarubral nucleus" in the deep intermediate stratum (sr; Fig. 8D). A significant number of CalR-IR neurons also appear at the more superficial intermediate stratum locus occupied by the parvicellular rubral primordium in p1 (ru; Figs. 8, 9).

Alar plate transition zone: Cytoarchitecture

We describe here in detail a distinct ventralmost part of the AP, identified as APtz in Figures 3–9. Typically, in p3 and p2, a cell-poor gap separates the ventricular zone from the periventricular zone in the APtz but is absent in the rest of the AP (Figs. 4–6), except caudally in p1, underneath the posterior commissure (Figs. 6–8). The APtz periventricular zone is occupied by a cell population that is markedly less dense than that appearing in this position in the rest of the alar plate (pv; APtz; Figs. 4–8). The APtz intermediate zone is separated from the periventricular zone by a layer of white matter, which includes the fibers of the posterior commissure in p1 that course into the tegmentum. The intermediate cellular layers in APtz is also less compact than its denser counterpart in the rest of the AP (Figs. 4–8), except at the commissural part of p1, where the AP intermediate zone becomes relatively less dense than that of the APtz (Fig. 9A). Finally, the superficial or marginal zone of APtz usually displays at all levels a small neuronal population, which is absent or less developed in the remaining AP. Comparative observations (Puelles, unpublished observations) suggest that a part of these superficial elements may be a primordium for the medial nucleus of the accessory optic tract, at least in p1.

Alar plate transition zone: CalR and CaBP immunoreactivity

CalR immunoreactivity is largely absent in the APtz, with the exception of some positive fibers in the white matter of the intermediate zone and some superficially placed neurons caudally in p1 (Figs. 9D, 10B). These seem to have reached this position, after crossing the BP marginal zone in the marginal migratory stream. A more complex pattern of distribution is observed for CaBP immunoreactivity. Distinct CaBP-IR cell populations segregate in the periventricular, intermediate, and superficial zones of the APtz, and there are also numerous labeled fibers, including the fiber bundles of the posterior commissure, longitudinally coursing fibers in the intermediate zone white matter, and the optic tract, which runs anteroposteriorly along the marginal stream of the AP. In p3, the

APtz periventricular zone shows only weak CaBP immunoreactivity (Figs. 4, 5). In contrast, the same zone in p2, p1, and midbrain shows a sizeable population of strongly CaBP-IR neurons (Figs. 6–10). The intermediate zone of APtz shows throughout abundant CaBP-IR fibers coursing longitudinally as well as a number of dispersed immunoreactive large neurons, particularly in its deeper half. Cells of this type are also found occasionally in the marginal zone.

TH immunoreactivity in the midbrain and diencephalic tegmentum

In this section, we relate the positions of TH-immunoreactive cells to the various FP, BP, and APtz subdivisions reported above, as detected in adjacent sections from the same stage 20 embryo.

Floor plate. TH-IR cell populations within the FP of p4 and p3 were sectioned somewhat obliquely (Figs. 3A, 4B,E, 5B,E; compare levels in Fig. 2). Nevertheless, these figures show that a subset of cells in the FP periventricular zone are TH immunoreactive; such cells are scarce in the FP intermediate zone of the mammillary pouch in p4 but clearly increase in number in p3 (Fig. 5B,E). The marginal zone of p3 already contains numerous TH-IR fibers coursing laterorostrally into the nigrostriatal tract (Fig. 5E, at the left side). In the FP of p2, the TH-IR cell bodies are found mainly in the intermediate zone; some of these have already advanced along the marginal migratory stream into the adjoining BPm column (1; Fig. 6E). The epichordal strip is practically devoid of TH-IR cells in p3 and p2. In contrast, the FP of p1 shows numerous TH-IR neurons within the periventricular and intermediate zones, with a gradient of increasing differentiation of this immunochemical profile as the cells acquire a more superficial position in the FP and enter the intermediate and marginal migratory streams into the BPm and BPl (1 and 2; Figs. 7B,E, 8B,E, 10C). The cells aggregated into a central mass around the p1 portion of the epichordal strip and are also strongly TH-IR (Figs. 7E, 8E, 10C). Some of the deeper positive cells in the periventricular zone seem to invade the gap separating the periventricular and intermediate strata of the BPm, converging at the origin of the intermediate migratory stream (Figs. 7, 8); others enter the intermediate stratum and exit laterally through the marginal migratory stream. At the midbrain/p1 transition, the marginal TH-IR migratory stream crosses all the BP and reaches laterally the APtz superficial zone (Figs. 9E, 10C).

All these features of TH expression in p1 are reproduced in the midbrain FP (Fig. 9), but not in the isthmus FP, whose width and cellularity diminishes rapidly, caudal to the isthmic fovea (if; Fig. 9A). There are only a few TH-IR neurons disposed obliquely or transversely across the isthmic FP; this gives the impression that these may have migrated caudally out of the midbrain FP and entered the isthmic region secondarily, although a local origin cannot be discounted. A small subset of deep TH-IR cells of the FP periventricular zone, also appear to migrate laterally into the space separating the ventricular and periventricular zones of the BPm in a "deep migratory stream" not detected with the other staining methods used here; these deep migrating cells are relatively more numerous at the caudal end of the midbrain (arrowhead at left; Fig. 9E).

Basal plate and alar transition zone. Apart from the TH-IR neurons forming part of the marginal and intermediate migratory streams (labeled 1 and 2, respectively, in Figs. 6–9), and the sparse cells forming the deep migratory stream, other TH-IR neurons with an apparent origin in the BPm of mes and p1–p3 are found in the BPm intermediate zone, usually adjacent to the FP/BP boundary (labeled 3 in the panels E of Figs. 4–9). These cells lie close to the intermediate migratory stream, with which they may eventually merge, as they are incorporated ventrolaterally into the SN/VTA. No TH-IR cells were found in the APtz, except at the caudal end of p1 (see above), as a result of the migratory advance of the marginal migratory stream. However, many TH-IR fibers aggregate into the mesotelencephalic pathway, initially occupy a superficial position in the BPl intermediate zone in mesencephalic and p1 segments (Figs. 7E, 8E), and then gradually course in the intermediate zone of the BP and APtz along the medial forebrain bundle (mfb) (Figs. 4E–6E).

GABA immunoreaction at stage 20

There is no GABA immunoreaction in the floor plate mantle zone or in the BPm. In the inner (deeper) sublayer of the BPl periventricular stratum, a few tangentially disposed GABA-IR neurons are present (panels F in Figs. 4–9). Groups of GABA-IR cells also are found in the BPl intermediate and marginal strata, with some local variation in their relative abundance, depending on the segmental level (BPl; panels B and F in Figs. 4–9). In p1, a GABA-IR group of the intermediate BPl coincides with the postulated anlage of the parvocellular red nucleus (ru; Figs. 8F, 9F). The putative anlage of the subthalamic nucleus in p4 (st; Figs. 4, 5) also shows GABA immunoreactivity at stage 20. GABA transporter (GAT-1) expression was detected in this nucleus in the adult human (Augood et al., 1999), but one cannot exclude a transient expression of GABA during development. GABA-IR neurons also are clearly present in the APtz, constituting separate populations in the periventricular, intermediate, and marginal strata (panels B and F in Figs. 4–9).

Comparison of TH- and GABA-immunoreactive populations at stage 18

The observation that GABA-IR neurons are found at stage 20 mainly within intermediate and marginal strata of the BPl and APtz prompted us to examine an earlier stage, with emphasis on the relations of such neurons with the TH-IR migratory streams. Figure 11 shows joint mappings of GABA-IR and TH-IR cells in representative cross-sections of the p3-mes continuum at stage 18 (Fig. 12). The GABA-IR cells are clearly present in the superficial mantle layer of the BPl and APtz longitudinal zones. TH-IR cells originating in the FP and BPm are distinct, particularly at p3 and p2 levels (Figs. 12A,B,C,D), and the marginal migratory stream is already well developed caudally (arrows, Fig. 11C; it is least developed in p3; Fig. 11A). The cells at the head of this stream enter the BPl marginal stratum in p2 and p1 and even approach the BPl/APtz boundary at midbrain levels. Here, they intermix with GABA-IR cells.

DISCUSSION

Longitudinal and radial organization of the mes-diencephalic tegmentum

Our earlier studies in human embryos identified an uninterrupted tegmental band of TH-IR neurons, which

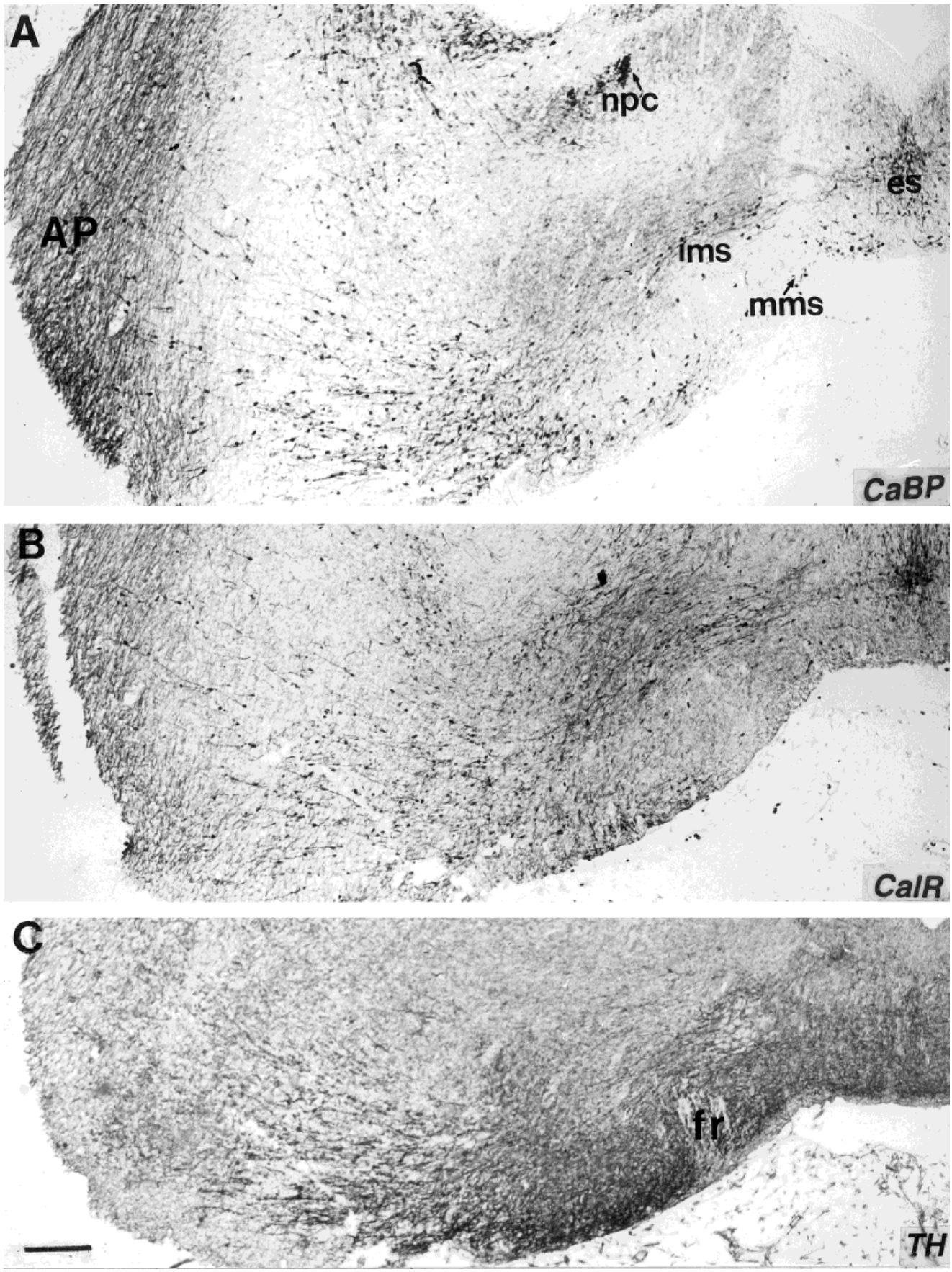

Fig. 10. Higher magnification photomicrographs of adjacent transverse sections of case N18 at the level of Figures 6, 7, immunostained with calbindin D28K (CaBP, **A**), calretinin (CalR; **B**), and tyrosine hydroxylase (TH; **C**) antibodies, respectively. The nucleus of the posterior commissure (npc in A) and the fasciculus retroflexus (fr) in C identify the level as characteristic of p1. Immunoreactive prospective SN neurons migrate laterally through the BP, along the intermediate and marginal migratory streams (ims, mms; note origin of these streams in the FP and BPm) and reach laterodorsally the alar plate (AP in A). Note higher density of CaBP and CalR immunoreactive cells at the FP central mass, centered at the epichordal strip (es in A). For other abbreviations, see list. Scale bar = 100 μm.

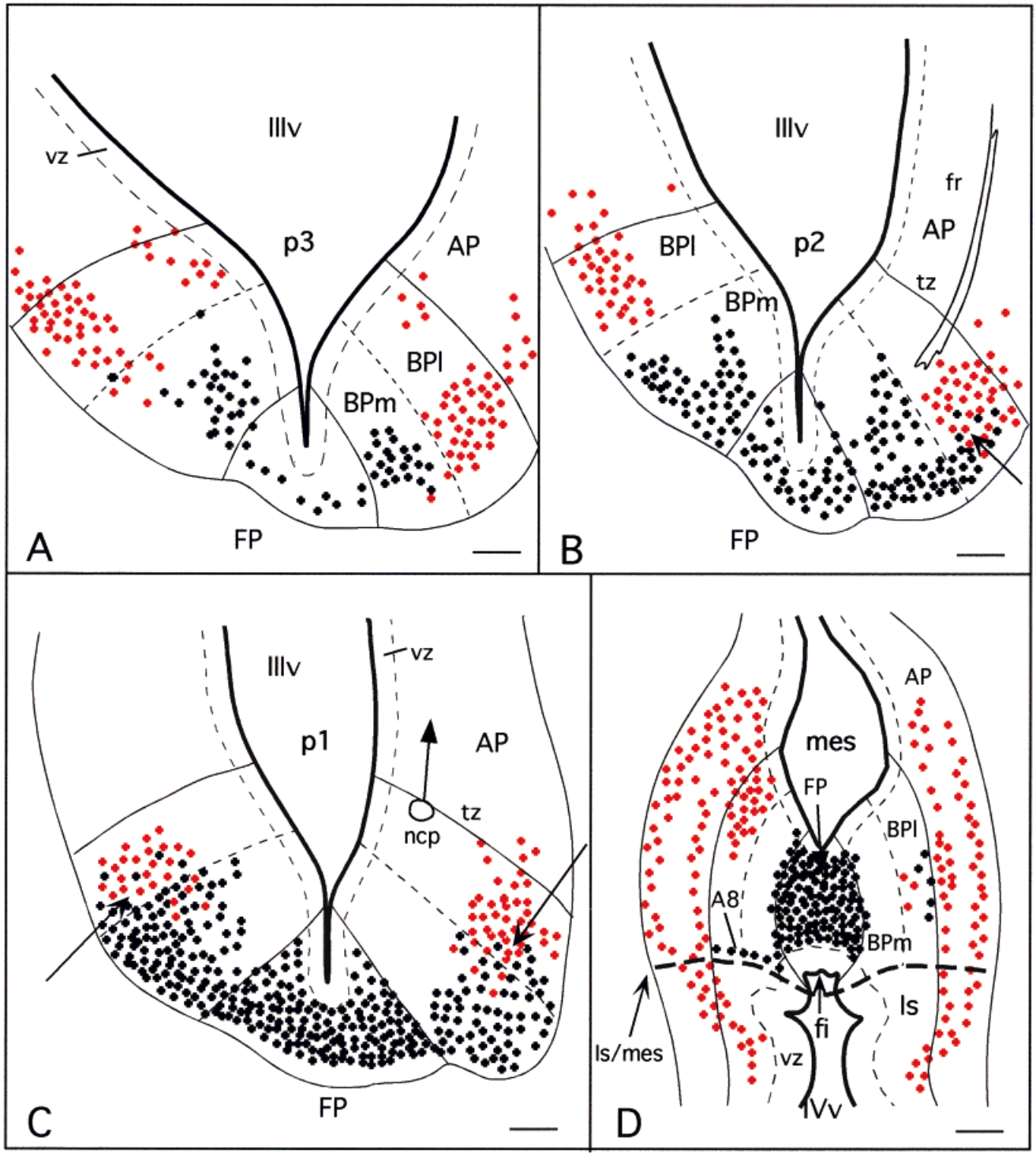

Fig. 11. **A–D:** Schematic drawings of tyrosine hydroxylase-immunoreactive (TH-IR; black dots) and γ-aminobutyric acid-immunoreactive (GABA-IR; red dots) neurons found in four transverse sections of the N19 (stage 18) specimen, which pass through the p3, p2, p1, and mes segments, respectively. The longitudinal FP, BPm, BPl, and AP zones are separated by continuous or dashed lines. Thick dashes indicate the isthmo-mesencephalic boundary in D. Note that the TH-IR neurons migrate already tangentially across the basal plate (arrows in B,C) and incipiently intermix with the GABA-IR neurons of the BPl, but not yet with those from the APtz. fi, isthmic fovea. For other abbreviations, see list. Scale bars = 100 μm in A–D.

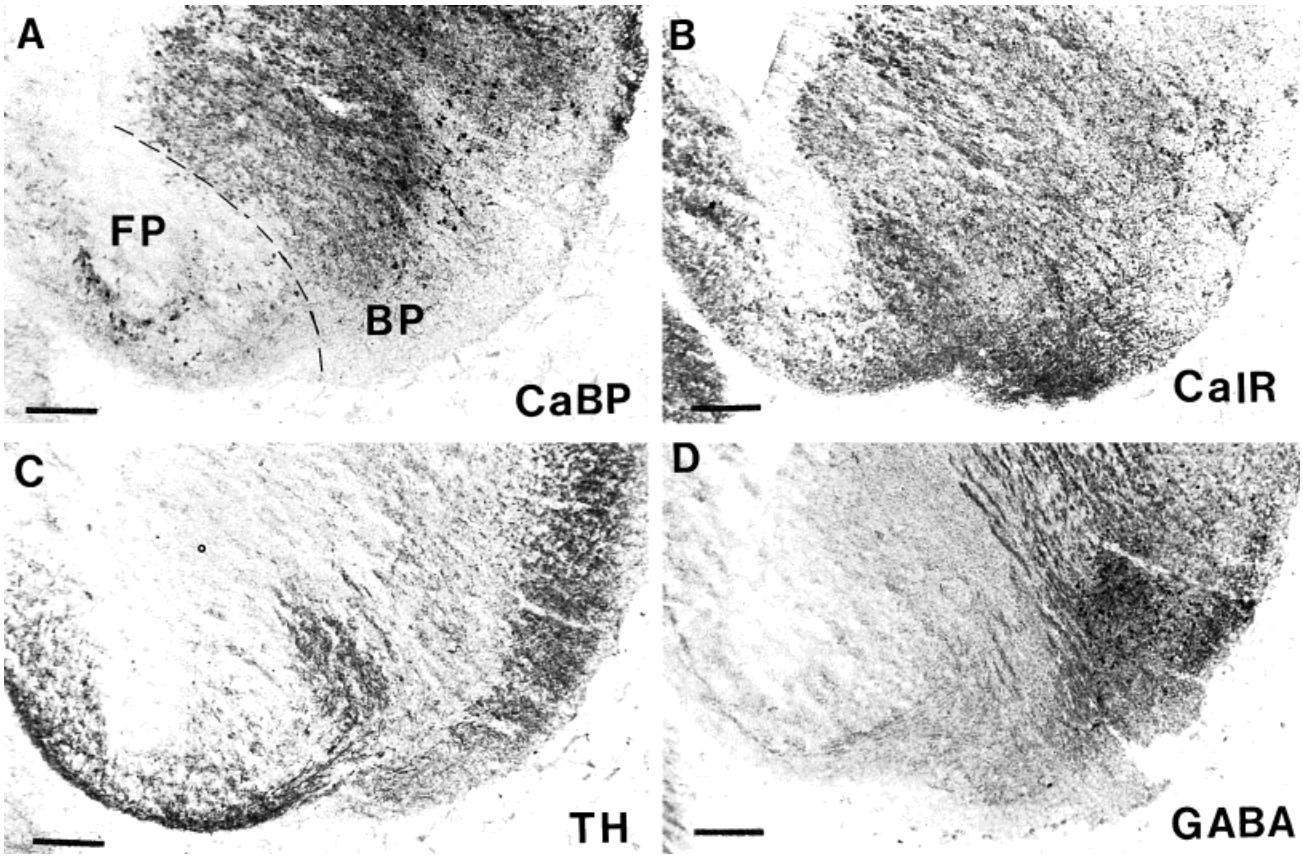

Fig. 12. Photomicrographs of transverse sections at the level of p3-p2 of the N19 embryo, showing immunolabeling with calbindin D28K (CaBP; **A**), calretinin (CalR; **B**), tyrosine hydroxylase (TH; **C**), and γ-aminobutyric acid (GABA; **D**) antibodies, corresponding to the drawing in Figure 11B. The dotted line delimits the floor plate (FP) from the basal plate (BP) in A. Note the distinct separate origin of a TH-immunoreactive (IR) (CaBP negative and CalR positive) cell group within the medial basal plate (C), as well as the incipient superficial migratory stream, contacting GABA-IR elements seen in D. Scale bars = 200 μm in A–D.

builds the mammalian SN and VTA from the isthmus to the retromammillary area (Zecevic and Verney, 1995; Puelles and Verney, 1998). The forebrain segmentation paradigm suggests that specific subpopulations of this continuum originate respectively in the isthmus, midbrain and the prosomeres p1–p3, apparently within their floor and basal plate domains (Puelles and Medina, 1994; Puelles and Verney, 1998). In the present study, we examined in more detail this last aspect, studying in cross-sections the cytoarchitecture and the CalR/CaBP/GABA-chemoarchitectural organization of the relevant longitudinal zones in human specimens at stages 18–22 and compared this with the location of TH-IR neurons. These data allowed us to differentiate various early neuronal populations, which were either confined to specific neural domains or distributed generally within particular zones. We found an unexpectedly rich variety of cell groups in the tegmental floor and basal plates, which vary in complexity, if not in size, with those found in the alar plate areas. We also obtained some preliminary data regarding the embryonic origin of the GABA-ergic neuronal population of the SN pars reticulata.

The floor plate. The rostral extent of the floor plate is a controversial point among different conceptions of the longitudinal organization of the brain. The orthodox view of Kingsbury (1920), recently restated by Kuhlenbeck (1973) and Marchand and Poirier (1983), defines the rostral limit of the FP as the rostral end of the fovea isthmi, at the midbrain-hindbrain junction. This makes the FP coextensive with the spinal cord and hindbrain midline raphe, which characteristically appears as a glycogen-rich, astroglial palisade (Vaage, 1969), in which there is little or no neuronal production (the raphe nuclei originate lateral to the FP itself; Lidov and Molliver, 1982; Wallace and Lauder, 1983). In this conventional view, all the ventral midline structures found on top of the cephalic flexure, rostral to the isthmus and up to the mammillary region (including SN and VTA), are, explicitely or explicitly, median basal plate derivatives of the midbrain (see Müller and O'Rahilly, 1989, 1990). However, Gilbert (1935) and Kahle (1956), studying human embryos, postulated the existence of a diencephalic tegmentum ventral to pretectum, dorsal thalamus, and ventral thalamus, and continuous with or forming a part of the subthalamus; these authors did not distinguish separate FP and BP domains.

His (1893) originally suggested that the FP extended to the rostral end of the neural tube, assigned by him to the retrochiasmatic recess. Recent studies using molecular markers, strongly suggested the existence of a modified

epichordal FP between the isthmus and the retromammillary region (Puelles et al., 1987; Shimamura et al., 1995), as well as a more drastically modified prechordal FP extending rostrally into the median eminence, as far as the retrochiasmatic recess (review in Puelles, 1995; Shimamura et al., 1995). Part of this mes-diencephalic epichordal FP is relevant to our study. In the mouse (and other vertebrates), this area exhibits early developmental expression of the gene Shh (Echelard et al., 1993; Roelink et al., 1994), and other characteristic FP genes, e.g. HNF-3β (Sasaki and Hogan, 1993; Ruiz i Altaba and Jessel, 1993) and annexin IV (Hamre et al., 1996; see Shimamura et al., 1995). Traditionally, the floor plate is thought to be composed of modified ependymal radial cells. Paramedian and median subpopulations of these FP cells can be identified immunocytochemically; these cells differ in marker content, notably vimentin, from adjacent BP and AP ependymal cells (Van Hartesveldt et al., 1986; Puelles et al., 1987; Stagaard and Mollgard, 1989; Mori et al., 1990; McKanna, 1992, 1993; Rodríguez et al., 1996). Our data indicate that a median epichordal strip is present in the human FP across the mes/p1–p3 continuum, essentially in agreement with the previous definition of this strip in the chick (Puelles et al., 1987).

The major phenotypic change observed in the midbrain and diencephalic (p1–p3) FP, compared with the isthmic and hindbrain FP, is the enlargement of the paramedian FP domains found on both sides of the epichordal strip; this enlargement is accompanied by considerable local production of neurons, a feature not readily observed in the hindbrain and spinal cord paramedian FP. Extended proliferative activity at this paramedian locus was reported by Müller and O'Rahilly (1989, 1990) in human embryos, although they attributed it to the midbrain.

The FP paramedian mantle zone recognized here first appears at stage 17, soon becomes incipiently divided into periventricular and intermediate strata (Fig. 7 in Lenn et al., 1978; Müller and O'Rahilly, 1989, 1990; present data at stages 18 and 20), and is clearly bilayered and shows the marginal migratory stream at stages 20–23 (Lenn et al., 1978; present data). Sections illustrated by Kahle (1956, his Fig. 5b) and Müller and O'Rahilly (1989, their Fig. 11D–F; 1990, their Fig. 11B,D) clearly display a bilayered subdivision (our periventricular and intermediate strata). Lenn et al. (1978) viewed this FP primordium as giving rise to the interpeduncular nucleus. Leaving aside the possible historical causes for this confusion, we concur with His' (1904) conclusion that the interpeduncular nucleus is a median formation of the rostral (isthmic) hindbrain, placed strictly ventral to the raphe nuclei formed in the isthmus and rhombomere-1. The interpeduncular nucleus accordingly lies entirely caudal to the midbrain as defined both by Palmgren (1921) and in the prosomeric schema followed here. In our interpretation, therefore, the results of Lenn et al. (1978) clearly refer to the FP derivatives in mes/p1–p2, including the primordium of the VTA and SN, and not to the interpeduncular nucleus. Müller and O'Rahilly (1989) attributed to the midbrain median proliferative zone the origin of both the substantia nigra, caudally (midbrain proper), and of the interpeduncular nucleus, rostrally (p1–p2; see comments above). Müller and O'Rahilly (1990) also designated cells at the rostral end of the epichordal FP anlage (just caudal to the mammillary pouch) as primordia for supramammillary and mammillary nuclei.

Apart from these confusing precedents found in the literature on human embryos, the reader may be referred to the study of Marchand and Poirier (1983) in the rat, in which they illustrated successive transverse sections across the midbrain and diencephalic tegmentum (all interpreted as purely mesencephalic). Early presence of a cell-poor epichordal glial strip can be observed in their Figures 3A–D, 4A–C, 5A–E, and 6A–E (it is later occluded by invading cells, as we observed here in human embryos). Paramedian neuronal populations appear on both sides of the epichordal strip, to a lesser but comparable extent than in human; these were called the medial streams of migrating cells. Accompanying ventrolateral streams of migrating cells were also described, which correspond to our basal plate populations and Gilbert's (1935) tegmentum. Curiously, both streams were presented as originating from the isthmus, although the isthmic fovea was correctly identified, caudal to the medial stream in their Figure 4D,E, and the clear documentation of the respective sectioning levels leaves no doubt that these "streams" are disposed uniformly and radially along the entire cephalic flexure, which suggests to us they originate locally. If these streams originated in the isthmus, then we would not expect the FP and BP neuroepithelium of midbrain and p1–p3 to produce any neuronal populations, a thesis that clearly does not agree with our data. Finally, the TH-immunoreactive material shown by Di Porzio et al. (1990) and Kawano et al. (1995), which also views the entire area as mesencephalic, suggests that a similar layered structure (periventricular, intermediate, and marginal strata) may be found at the relevant midbrain and diencephalic FP domains in mice.

This remarkable paramedian FP matrix area is obviously an important site where prospective dopaminergic SN and VTA neurons are produced. That different subpopulations across the two strata are immunoreactive for CalR, CaBP, or TH (none to GABA), whereas a surplus of cells seems to remain uncharacterized by these three markers, suggests that the paramedian FP also contributes to other neighboring formations. Available atlases of the mouse or rat brain are somewhat vague regarding this particular area. However, other nuclei that may be recipient of some of these FP cells are the anteromedial nucleus (Leichnetz, 1982; Phipps et al., 1983), the central linear nucleus, the interfascicular nucleus, the paranigral nucleus, the parapeduncular nucleus, and the parabrachial pigmented nucleus (Paxinos et al., 1991; McRitchie et al., 1996; Lewis and Sesack, 1997). Part of the "supramammillary nucleus" complex, formed across the FP and BP of p3 (called "retromammillary area" in the prosomeric model; Puelles, 1995) may also be included with these "recipient" nuclei.

Development of a modified epichordal FP rostral to the rhombencephalic isthmus seems to be due to a variant of the ventralizing induction effect, which is initiated at the rostral end of the notochord in concert with sonic hedgehog (Shh) signaling. This mechanism probably mediates as well the particular morphogenesis of the local BP, by inhibiting the effects of counteracting dorsalizing developmental genes (Yamada et al., 1993; Hatta et al., 1994; Jessell and Lumsden, 1997). It is significant that ectopic overexpression of Pax3 (normally an alar marker; Stoykova and Gruss, 1994) at the ventral midline was associated with the absence of FP differentiation (Tremblay et al., 1996). More work is needed to understand the

cascade of gene effects involved in the differentiation of this plurisegmental FP region and the histogenetic differences observed in the mes-diencephalic FP domain with respect to both hindbrain/spinal cord FP and the rostral prechordal FP in the median floor of the hypothalamus (Puelles, 1995).

The basal plate. For historical reasons briefly considered in the Introduction section, little attention was given in the past to the detailed structure of the diencephalic basal plate in any species, resulting in a dearth of primary data, illustrations, or even schematic interpretations; the relevant developmental concepts are dominated by midbrain-centered descriptions and assumptions of doubtful validity. A systematic study nevertheless can be undertaken using the prosomeric approach (Puelles, 1995; Shimamura et al., 1995; Puelles and Verney, 1998), as shown in the present work. The concept of a diencephalic basal plate in p3, p2, and p1, which is strictly continuous with the midbrain counterpart and colinear with the corresponding FP, is strongly supported by the expression of developmental genes such as shh, HNF-3β, Nkx-6.1, Sim-1, Isl-1, and MP20 in the mouse or chick (Sasaki and Hogan, 1994; Shimamura et al., 1995; Ericson et al., 1995; Timsit et al., 1995; Fan et al., 1996; Qiu et al., 1998). A common alar/basal boundary can be delineated with the neuroepithelial expression of Pax3, Pax-6, and Pax7 and other genes in the alar plate (Stoykova and Gruss, 1994; Schubert et al., 1995); a longitudinal stripe of Nkx-2.2 expression approximates the position of the alar/basal limit (Shimamura et al., 1995). In addition, present data show that, in human embryos, CalR immunoreaction characterizes this BP domain, by virtue of expression in the BP periventricular stratum neurons and their radial processes, which spread into the intermediate zone. Immunoreaction for CaBP also appears generally in the BP, except in p1.

Our division of the BP cytoarchitectural schema into medial and lateral parts (BPm, BPl), each subdivided into ventricular, periventricular, intermediate, and marginal strata, agrees with earlier embryologic observations of Palmgren (1921) and Rendahl (1924) in diverse vertebrate brains. This schema is supported by our Nissl data, as well as by the CalR and CaBP immunocytochemical observations, and is also supported by our mapping of GABA-IR neurons in diverse strata of BPl and APtz (although not in BPm). It is difficult to relate our results to previous studies, because transverse sections through the diencephalic BP of human embryos are rarely reported in the literature. However, we found that a Nissl section illustrated by Kahle (1956) in his Figure 5b is comparable to our Figure 5 (the stage of mantle differentiation also seems similar, although the age given is more advanced). The structure of the FP, BP, and adjacent APtz observed in this photomicrograph strictly corroborates our observations in human embryos. Müller and O'Rahilly (1990) also show one section that is transverse to the caudal diencephalic tegmentum in a younger, stage 17 human embryo (their Fig. 9B). Apart from the clearly distinct FP and BP regions, the domain identified by us as APtz is marked in that figure with an arrowhead and said in the legend to indicate the primordium of the subthalamic nucleus (see our Figs. 4, 5 for our interpretation of where this primordium lies); this "APtz" clearly stands out from the BP and merges with, but remains distinct from, the rest of the AP. Gribnau and Geijsberts (1985) show a section transverse to the midbrain in a stage 20 rhesus monkey embryo (their Fig. 11G); the observed structure of the FP and BP, although not commented upon by these authors, also agrees with our present results. Data found at relevant loci in a variety of developmental atlases of mouse and rat embryos suggest that the referred structural schema of the diencephalic and midbrain BP may be general, at least in mammals.

As a collateral result of our study, we concluded that the parvicellular nucleus ruber actually lies outside the midbrain proper and is presumably represented by a group of cells (including GABA-IR ones) in the superficial half of the BPl intermediate stratum of p1 (pretectum). This conclusion is supported by the constant reference in the literature to its rostral boundary coinciding with the vertical course of the retroflex tract. The "suprarubral nucleus," whose CalR-IR neurons lie deep to the parvicellular nucleus ruber, may have been interpreted by other authors as a lateral part of the interstitial nucleus of Cajal. The so-called "rostral interstitial nucleus" occupies a similar position within the BPl of p2, rostral to the retroflex tract (compare Büttner-Enever and Büttner, 1978). Still deeper, CaBP immunoreactivity highlights the cells and commissural axons of the basal nucleus of the posterior commissure. This cell group is found within the deep BPl intermediate stratum of p1, whereas Cajal's interstitial nucleus, or nucleus of the medial longitudinal fasciculus (also in p1) is dispersed in the BPl intermediate stratum, and the nuclei of Darkschewitsch and Bechterew are found in the BPm periventricular stratum (Leichnetz, 1982; Leichnetz et al., 1984). The remaining, disperse BP cell populations of the intermediate stratum build a pretectal and subthalamic (or posterior hypothalamic) reticular formation, whereas the denser periventricular stratum participates in the periaqueductal gray, which may be stretched conceivably as far rostrally as the posterior limit of the mammillary region (p3/p4 boundary).

The alar plate transition zone. This structurally distinct domain appears ventrally within the alar plate. We include it in the alar plate because of similarities observed in (1) the relative thickness (inverse of exhaustion rate) of the ventricular zone, (2) cell layering and relative density of the individual strata, and (3) CaBP- and GABA-immunoreaction patterns. An overall ventrodorsal gradient of AP mantle layer differentiation (also suggested by some neurogenetic data in the literature), in addition to a greater density of longitudinally coursing fibers in the APtz, may explain some of the cytoarchitectural differences observed between APtz and the rest of AP. We cannot exclude the possibility that there may be qualitative differences between these neuronal populations i.e., that some may only be present within the APtz and not in the rest of the AP (suggested perhaps by the local end of the SN tangential migration). Although a precise correlation with developmental genes expressed either in the BP or AP is not yet available in any species, we suggest that the APtz expresses alar marker genes (i.e., Pax-6), and probably lies adjacent lateral to the alar/basal boundary-associated expression of Nkx-2.2 (Puelles and Rubenstein, 1993; Shimamura et al., 1995).

Development of the SN/VTA TH-immunoreactive cell groups

As concluded in earlier publications (Puelles and Medina, 1994; Puelles and Verney, 1998), the rostral portions

of the SN/VTA complex develop in the caudal diencephalon. Many illustrations found in the literature on the SN/VTA complex, under the assumption that they represent midbrain sections, actually display sections through this diencephalic portion. As a rule of thumb, all cross-sections in which the oculomotor nucleus is absent belong to the diencephalic p1–p3 tegmentum (see Specht et al., 1981; Altman and Bayer, 1981; Levitt and Rakic, 1982; Marchand and Poirier, 1983; Voorn et al., 1988; Di Porzio et al., 1990; Schultz et al., 1990; Verney et al., 1991; Freeman et al., 1991; Kawano et al., 1995; Zecevic and Verney, 1995; Almqvist et al., 1996).

Our results show that the TH-IR dopaminergic cell groups A9–A10 are generated specifically in the FP of the midbrain and prosomeres p1–p3, with a collateral contribution of the contiguous BPm. This pattern of early histogenesis is consistent with numerous descriptions in primates and rodents, although our study seems to be the first that describes the FP and BPm. In vitro studies have suggested that the induction of the SN/VTA dopaminergic phenotype is a function of Sonic hedgehog protein secreted at the mesencephalic floor plate, acting upon differentiation capacities generated by other local genes (Wang et al., 1995; Hynes et al., 1995a,b; Perrone-Capano and di Porzio, 1996; Hynes and Rosenthal, 1999). One background gene plausibly implicated in this discrimination may be Otx2, which has a distinct caudal boundary at the isthmomesencephalic boundary (Simeone et al., 1992). The *Shh* protein is also secreted by the notochord and hindbrain floor plate, without elliciting the dopaminergic phenotype; however, the spinal cord does develop a population of dopaminergic cells adjacent to its floor plate (Pindzola et al., 1990; Smeets and Reiner, 1994).

Induction of the dopaminergic phenotype by Shh protein, although usually attributed to the mesencephalon, obviously occurs also in the contiguous p1–p3 segments, where this ventralizing protein is also present (Echelard et al., 1993; Shimamura et al., 1995; Ericson et al., 1995). In fact, detailed mappings show that Shh is expressed at very early stages in the floor plate and then in the midbrain and p1–p3 basal plate, whilst the FP signal diminishes (Shimamura et al., 1995). This sequence may correlate with the observed production of dopaminergic neurons both in the FP and BPm. Differences between the genetic make-up of the brain segments may give rise to peculiarities of the dopaminergic cell populations produced at each rostrocaudal level. Indeed, in the adult human, the dopamine-containing neurons located rostrally in the SN are more resistant to the cell death process occurring in Parkinson's disease than those located caudally (Matzuk and Saper, 1985; Damier et al., 1999).

Another gene critical for the differentiation of normal SN/VTA dopaminergic neurons is Nurr-1 (coding for an orphan member of the steroid/thyroid hormone receptor family), which normally is expressed in the early SN/VTA FB/BP continuum, approximately 1 day earlier than the appearance of TH immunoreaction. Null mice mutants for this gene selectively lack the SN/VTA cell populations and die shortly after birth with a hypoactivity syndrome. This receptor can form heterodimers with the 9-cis retinoic acid receptor (RXR), which suggests a potential role of retinoids in controlling this differentiation route, perhaps inhibiting it in the hindbrain (Zetterström et al., 1997).

One aspect revealed in our study is the unequal density of TH-, CalR-, and CaBP-immunoreactive neurons differentiating in the FP. Irrespective of the segmental level, maximal numbers of any of these neuronal types occur medially in the paramedian periventricular zone of the FP. At some places, dense central aggregates form at the midline occupied by the epichordal strip of the FP. This pattern suggests that epichordal FP ependymal cells may be fundamentally important for the specification of these phenotypes, or at least may release molecules stimulating differentiation and migration of these cells. A direct effect of midbrain FP astroglia on induction of the dopaminergic phenotype (Beyer et al., 1991; perhaps through Shh), or affecting the cell shape and possibly the migratory properties of the differentiating dopaminergic neurons, was reported (Denis-Donini et al., 1984; Rousselet et al., 1990).

After they are generated, TH-IR neurons apparently migrate radially, obliquely, or tangentially within the intermediate and marginal migratory streams, to reach the BP and APtz marginal tegmentum, as observed in cross-sections and sagittal sections by us and others (Di Porzio et al., 1990; Schultz et al., 1990; Verney et al., 1991; Kawano et al., 1995). This migration out of the FP may obey an as yet poorly studied repellent guidance mechanism; the brain floor plate is known to release molecules that repel growing axons (Colamarino and Tessier-Lavigne, 1995; Tamada et al., 1995; Guthrie and Pini, 1995). One of these molecules, netrin-1, is strongly expressed in the midbrain and caudal diencephalic FP, particularly at and around the epichordal strip. It also appears more weakly in the BPm ventricular zone and mantle layer, as well as in the intermediate and superficial migratory stream primordia of the SN/VTA (Livesey and Hunt, 1997; see their Fig. 5A,B).

Progressive rostrocaudal and mediolateral unfolding of the superficially migrating TH-, CaBP- and CalR-IR neuronal populations (these seem largely overlapping in extent and density) gradually builds up the anlage of the SN pars compacta and the VTA. This pattern of migration observed in human embryos possibly corresponds to the rostrocaudal gradient of neurogenesis described in rodents (Altman and Bayer, 1981; Specht et al., 1981; Voorn et al., 1988). The earliest generated populations apparently migrate obliquely and laterally within p1–p2 and may correspond specifically to the lateral SN component described in the adult brain (Solberg et al., 1993). Neurons migrating later possibly tend to aggregate more medially, leaving the youngest cells in the VTA. Such a temporally and spatially modulated pattern of SN migration may relate ultimately to the adult lateromedial and dorsoventral functional organization of the complex (van Domburg and ten Donkelaar, 1991; Solberg et al., 1993). Indeed, it might be possible to relate the intermediate migratory stream and associated cells originated in the neighboring BPm to the dorsal part (or tier) described in the monkey and human SN pars compacta, and eventually even to distinct cell groupings within this area (review in Lewis and Sesack, 1997). The superficial migratory stream seems topographically more related to the ventral part or tier of the SNc and VTA (Fig. 10). Finally, the deep migratory stream seems a clear candidate for the origin of the periaqueductal dopaminergic cell population and possibly also for the A8 dopaminergic cell group (see our Figs. 9E, 11, 12).

Development of the putative substantia nigra pars reticulata

Data on the development of the SN mention similar birthdates for neurons of the substantia nigra pars compacta comprising DA neurons and of the substantia nigra pars reticulata (Altman and Bayer, 1981; Levitt and Rakic, 1982). Most neurons in the SN pars reticulata use the inhibitory neurotransmitter GABA in the adult brain, as shown by immunostaining by using antibodies directed against the GABA-synthetizing enzyme glutamate decarboxylase (GAD) (Oertel et al., 1982). In an effort to study in parallel the development of both components of the SN, we mapped GABA-positive neurons in our material at stages 18 and 20. Such cells were detected in the lateral basal plate of the p3, p2, and p1 segments, as well as in the adjoining alar plate transition zone. As shown in Figure 12, at stage 18, GABA-IR young neurons migrate radially toward the brain surface within the BPl and APtz; these cells are approached from medially by TH-IR (as well as CaBP-IR and CalR-IR) neurons arising from the FP through the intermediate and superficial migratory streams. At stage 20, the GABA-positive populations in the BPl and APtz are still present, and the TH-IR migrating cells have intermixed with the BPl cells and begin to penetrate the GABA-positive marginal stratum of the APtz. This pattern suggests that the SN pars reticulata neurons may originate at least in the BPl, but perhaps also in the adjoining APtz.

GABA-immunoreactive elements were also studied in the developing rat brain (Lauder et al., 1986), with results in sagittal sections essentially consistent with ours, although transverse sections through the mes-p1-p3 domain were not shown, hindering detailed comparison. These immunochemical observations nevertheless need to be interpreted with caution, since GABA expression can be transient during development and does not necessarily mean long-term differentiation of the GABAergic phenotype, or synthesis of GABA. GABA may transiently regulate proliferatory or migratory processes during development (Rozenberg et al., 1989; LaMantia, 1995; Lo Turco et al., 1995). It can be taken up from the extracellular matrix and expressed transiently in some neuronal populations (Meinecke and Rakic, 1992). Nevertheless, the distribution of GAD67 mRNA in developing rat embryos (GAD67 is one of the two enzyme isoforms synthetizing GABA in adults) reveals a tegmental band stretching longitudinally from the midbrain to the subthalamus, roughly coinciding in position with our PBl and APtz. Unfortunately, absence of transverse sections through our region of interest prevents a direct correlation with our results (Behar et al., 1994). Early GAD67 transcripts may be differentially spliced, including an exon with a premature stop codon, which theoretically prevents the enzyme from functioning (Bond et al., 1990). Such transcripts may coexist with functional ones (Behar et al., 1994). It is as yet unclear how this relates to the immunodetected GABA.

ACKNOWLEDGMENTS

We thank Dr. A. Vigny who gave us the anti-TH antibodies, A. Muzerelle, and C. Alvarez for excellent technical work and D. Le Cren for photographic work. C.V. and N.Z. were supported by INSERM, ECC, and L.P. received a grant from CICYT.

LITERATURE CITED

Almqvist PM, Akesson E, Wahlberg LU, Pschera H, Seiger A, Sundstrom E. 1996. First trimester of the human nigrostriatal dopamine system. Exp Neurol 139:227–237.

Altman J, Bayer SA. 1981. Development of the brain stem in the rat: V. Thymidine-radiographic study of the time of origin of neurons in the midbrain tegmentum. J Comp Neurol 198:677–716.

Augood SJ, Waldvogel HJ, Munkle MC, Faull RL, Emson PC. 1999. Localization of calcium-binding proteins and GABA transporter (GAT-1) messenger RNA in the human subthalamic nucleus. Neuroscience 88: 521–534.

Behar T, Ma W, Hudson L, Barker JL. 1994. Analysis of the anatomical distribution of GAD67 mRNA encoding truncated glutamic acid decarboxylase proteins in the embryonic rat brain. Brain Res Dev Brain Res 77:77–87.

Beyer C, Pilgrim C, Reisert I, Misgeld U. 1991. Cells from embryonic rat striatum cocultured with mesencephalic glia express dopaminergic phenotypes. Neurosci Lett 128:1–3.

Bond RW, Wyborski RJ, Gottlieb DI. 1990. Developmentally regulated expression of an exon containing a stop codon in the gene for glutamic acid decarboxylase. Proc Natl Acad Sci USA 87:8771–8775.

Büttner-Enever JA, Büttner U. 1978. A cell group associated with vertical eye movements in the rostral mesencephalic reticular formation of the monkey. Brain Res 151:31–47.

Colamarino SA, Tessier-Lavigne M. 1995. The axonal chemoattractant netrin-1 is also a chemorepellent for trochlear motor axons. Cell 81: 621–629.

Damier P, Hirsch EC, Agid Y, Graybiel AM. 1999. The substantia nigra of the human brain: II. Patterns of loss of dopamine-containing neurons in Parkinson's disease. Brain 122:1437–1448.

Denis-Donini S, Glowinski J, Prochiantz A. 1984. Glial heterogeneity may define the three dimensional shape of mouse mesencephalic dopaminergic neurons. Nature 307:641–643.

Dahlström A, Fuxe K. 1964. Evidence for the existence of monoamine-containing neurons in the central nervous system: I. Demonstration of monoamines in the cell bodies of the brain stem neurons. Acta Physiol 232:(Suppl 62) 1–55.

Di Porzio U, Zuddas A, Cosenza-Murphy DB, Barker JL. 1990. Early appearance of tyrosine hydroxylase immunoreactive cells in the mesencephalon of mouse embryos. Int J Dev Neurosci 8:523–532.

Echelard Y, Epstein DJ, St-Jacques B, Shen L, Mohler J, Mc Mahon JA, Mc Mahon AP. 1993. Sonic hedgehog, a member of ta family of putative signaling molecules, is implicated in the regulation of CNS polarity. Cell 75:1417–1430.

Ericson J, Muhr J, Placzek M, Lints T, Jessell TM, Edlund T. 1995. Sonic hedgehog induces the differentiation of ventral forebrain neurons: a common signal for ventral patterning within the neural tube. Cell 81:747–756.

Fan CM, Kuwana E, Bulfone A, Fletcher CF, Copeland NG, Jenkins NA, Martínez S, Puelles L, Rubenstein JLR, Tessier-Lavigne M. 1996. Expression patterns of two murine homologs of *Drosophila* single-minded suggest possible roles in embryonic patterning and in the pathogenesis of Down syndrome. Mol Cell Neurosci 7:1–16.

Freeman TB, Spence MS, Boss BD, Spector DH, Strecker RE, Olanow WC, Kordower JH. 1991. Development of dopaminergic neurons in the human substantia nigra. Exp Neurol 113:344–353.

Gilbert MS. 1935. The early development of human diencephalon. J Comp Neurol 62:81–115.

Gribnau AAM, Geijsberts LGM. 1985. Morphogenesis of the brain in staged Rhesus monkey embryos. Adv Anat Embryol Cell Biol 91:1–69.

Guthrie S, Pini A. 1995. Chemorepulsion of developing motor axons by the floor plate. Neuron 14:1117–1130.

Hamre KM, Keller-Peck CR, Campbell RM, Peterson AC, Mullen RJ, Goldowitz D. 1996. Annexin IV is a marker of roof and floor plate development in the murine CNS. J Comp Neurol 368:527–537.

Hatta K, Puschel AW, Kimmel CB. 1994. Midline signaling in the primordium of the zebrafish anterior central nervous system. Proc Natl Acad Sci USA 91:2061–2065.

His, W. 1893. Vorschläge zur Eintheilung des Gehirns. Arch Anat Entwicklungsgesch Leipzig 17:172–179.

His, W. 1904. Die Eintheilung des menschlichen Gehirns während der ersten Monate. Leipzisg: S Hirzel Verlag.

Hynes M, Poulsen M, Tessier-Lavigne M, Rosenthal M. 1995a. Control of

neuronal diversity by the floor plate: contact-mediated induction of midbrain dopaminergic neurons. Cell 80:95–101.

Hynes M, Porter JA, Chiang C, Chang D, Tessier-Lavigne M, Beachy PA, Rosenthal A. 1995b. Induction of midbrain dopaminergic neurons by sonic hedgehog. Neuron 15:35–44.

Hynes M, Rosenthal A. 1999. Specification of dopaminergic neurons: inductive factors and their receptors. In: di Porzio U, Pernas-Alonso R, Perrone-Capano C, editors. The development of dopaminergic neurons. Austin, TX: R. G. Landes Co. p 15–35.

Jacobowitz DM, Abbott LC. 1998. Chemoarchitectonic atlas of the developing mouse brain. New York: CRC Press LLC.

Jessell TM, Lumsden A. 1997. Inductive signals and the assignment of cell fate in the spinal cord and hindbrain. In: Cowan WM, Jessell TM, Zipursky SL, editors. Molecular and cellular approaches to neural development. New York: Oxford University Press. p 290–333.

Kahle WF. 1956. Zur Entwicklung des menschlichen Zwischenhirs. Detsch Z Nervenheidlkd 175:259–318.

Kawano H, Ohyama K, Kawamura K, Nagatsu I. 1995. Migration of dopaminergic neurons in the embryonic mesencephalon of mice. Brain Res Dev Brain Res 86:101–113.

Keyser A. 1972. The development of the diencephalon of the chinese hamster. An investigation of the validity of the criteria of subdivision of the brain. Acta Anat Suppl (Basel) 59:1–178.

Kingsbury BF. 1920. The extent of the floor-plate of His and its significance. J Comp Neurol 32:113–135.

Kuhlenbeck H. 1973. Neuromery, definitive main subdivision. The central nervous system of the vertebrates. Vol. 3, Part 2: Overall morphologic pattern. Basel: Karger. p 304–350.

LaMantia AS. 1995. The usual uspects: GABA and glutamate may regulate proliferation in the cortex. Neuron 15:1223–1225.

Lauder JM, Han VKM, Henderson P, Verdoorn T, Towle AC. 1986. Prenatal ontogeny of the GABAergic system in the rat brain: an immunocytochemical study. Neuroscience 19:465–493.

Leichnetz GR. 1982. The medial accessory nucleus of Bechterew: a cell group within the anatomical limits of the rostral oculomotor complex receives a direct prefrontal projection in the monkey. J Comp Neurol 210:147–151.

Leichnetz GR, Spencer RF, Smith DJ. 1984. Cortical projections to nuclei adjacent to the oculomotor complex in the medial dien-mesencephalic tegmentum in the monkey. J Comp Neurol 228:359–387.

Lenn NJ, Halfon N, Rakic P. 1978. Development of the interpeduncular nucleus in the midbrain of Rhesus monkey and human. Anat Embryol (Berl) 152:273–289.

Levitt P, Rakic P. 1982. The time of genesis, embryonic origin and differentiation of the brain stem monoamine neurons in the rhesus monkey. Brain Res Dev Brain Res 4:35–57.

Lewis DA, Sesack SR. 1997. Dopamine systems in the primate brain. In: Bloom FE, Björklund A, Hökfelt T, editors. Handbook of chemical neuroanatomy, Vol. 13. The primate nervous system, Part I. Amsterdam: Elsevier. p 263–376.

Lidov HG, Molliver ME. 1982. Immunohistochemical study of the development of serotoninergic neurons in the rat CNS. Brain Res Bull 9:559–604.

Livesey FJ, Hunt SP. 1997. Netrin and netrin receptor expression in the embryonic mammalian nervous system suggests roles in retinal, striatal, nigral, and cerebellar development. Mol Cell Neurosci 8:417–429.

Lo Turco JJ, Owens DF, Heath MJ, Davis MB, Kriegstein AR. 1995. GABA and glutamate depolarize progenitor cells and inhibit DNA synthesis. Neuron 15:1287–1298.

McKanna JA. 1992. Optic chiasm and infundibular decussation sites in the developing rat diencephalon are defined by glial raphes expressing p35. lipocortin 1, annexin I. Dev Dyn 195:75–86.

McKanna JA. 1993. Primitive glial compartments in the floor plate of mammalian embryos: distinct progenitors of adult astrocytes and microglia support the notoplate hypothesis. Perspect Dev Neurobiol 1:245–255.

McRitchie DA, Hardman CD, Halliday GM. 1996. Cytoarchitectural distribution of calcium binding proteins in midbrain dopaminergic regions of rats and humans. J Comp Neurol 364:121–150.

Marchand R, Poirier LJ. 1983. Isthmic origin of neurons of the rat substantia nigra. Neuroscience 9:373–381.

Matzuk MM, Saper CB. 1985. Preservation of hypothalamic dopaminergic neurons in Parkinson's disease. Ann Neurol 18:552–555.

Meinecke DL, Rakic P. 1992. Expression of GABA and GABAA receptors by neurons of the subplate zone in developing primate occipital cortex. J Comp Neurol 317:91–101.

Mori K, Ikeda J, Hayaishi O. 1990. Monoclonal antibody R2D5 reveals midsagittal radial glial system in postnatally developing and adult brainstem. Proc Nat Acad Sci USA 87:5489–5493.

Muller F, O'Rahilly R. 1989. The human brain at stages 17, including the appearance of the future olfactory bulb and the first amygdaloid nuclei. Anat Embryol (Berl) 180:353–369.

Muller F, O'Rahilly R. 1990. The human brain at stages 18–20, including the choroid plexuses and the amydaloid and septal nuclei. Anat Embryol (Berl) 182:285–306.

Muller F, O'Rahilly R. 1994. Occipitocervical segmentation in staged human embryos. J Anat 185:251–258.

Nieuwenhuys R. 1998. Morphogenesis and general structure. In: Nieuwenhuys R, ten Donkelaar HT, Nicholson C, editors. The central nervous system of vertebrates. Berlin: Springer. p 158–228.

Oertel WH, Tappaz ML, Berod A, Mugnaini E. 1982. Two-color immunohistochemistry for dopamine and GABA neurons in the rat substantia nigra and zona incerta. Brain Res Bull 9:463–474.

Palmgren A. 1921. Embryological and morphological studies on the midbrain and cerebellum of vertebrates. Acta Zool (Stockh) 2:1–94.

Paxinos G, Törk I, Tecott LH, Valentino KL. 1991. Atlas of the developing rat embryo. San Diego: Academic Press.

Perrone-Capano C, di Porzio U. 1996. Epigenetic factors and midbrain dopaminergic neurone development. Bioessays 18:1–8.

Phipps BS, Maciewicz R, Sandrew BB, Poletti CE, Foote WE. 1983. Edinger-Westphal neurons that project to spinal cord contain substance P. Neurosci Lett 36:125–131.

Pindzola RR, Ho RH, Martin GE. 1990. Development of catecholaminergic projections to the spinal cord in the North American opossum, *Didelphis virginiana.* J Comp Neurol 294:399–417.

Puelles L. 1995. A segmental morphological paradigm for understanding vertebrate forebrains. Brain Behav Evol 46:319–337.

Puelles L, Medina L. 1994. Development of neurons expressing tyrosine hydroxylase and dopamine in the chicken brain: a comparative segmental analysis. In: Smeets WJAJ, Reiner A, editors. Phylogeny and development of catecholamine systems in the CNS of vertebrates. Cambridge, UK: Cambridge University Press. p 381–401.

Puelles L, Rubenstein JLR. 1993. Expression patterns of homeobox and other putative regulatory genes in the embryonic mouse forebrain suggest a neuromeric organization. Trends Neurosci 16:472–476.

Puelles L, Verney C. 1998. Early neuromeric distribution of tyrosine-immunoreactive neurons in human embryos. J Comp Neurol 394:283–308.

Puelles L, Amat JA, Martinez-de-la-Torre M. 1987. Segment-related, mosaic neurogenetic pattern in the forebrain and mesencephalon of early chick embryos: I. Topography of AChE-positive neuroblasts up to stage HH18. J Comp Neurol 266:247–268.

Qiu M, Shimamura K, Sussel L, Chen S, Rubenstein JLR. 1998. Control of anteroposterior and dorsoventral domains of Nkx-6 1 gene expression relative to other Nkx genes during vertebrate CNS development. Mech Dev 72:77–88.

Rendahl H. 1924. Embryologische und morphologische Studien über das Zwischenhirn beim Huhn. Acta Zool (Stockh) 5:241–344.

Rodríguez EM, Del Brio León MA, Riera P, Menéndez J, Schoebitz K. 1996. The floor plate of the hindbrain is a highly specialized gland: Immunocytochemical and ultrastructural characteristics. Brain Res Dev Brain Res 97:153–168.

Roelink H, Augsberger A, Heemskerk J, Korzh V, Norlin A, Ruiz i Altaba A, Tanabe A, Placzek M, Edlund T, Jessell T, Dodd J. 1994. Floor plate and motor neuron induction by vhh-1, a vertebrate homolog of hedgehog expressed in the notochord. Cell 76:761–775.

Rousselet A, Autilio-Touati A, Araud D, Prochiantz A. 1990. In vitro regulation of neuronal morphogenesis and polarity by astrocyte-derived factors. Dev Biol 137:33–45.

Rozenberg F, Robain O, Jardin L, Ben-Ari Y. 1989. Distribution of GABAergic neurons in late fetal and early postnatal rat hippocampus. Brain Res 50:177–187.

Ruiz i Altaba A, Jessell TM. 1993. Midline cells and the organization of vertebrate neuroaxis. Curr Opin Gen Dev 3:633–640.

Sasaki H, Hogan BLM. 1994. HNF-3b as a regulator of floor plate development. Cell 76:103–115.

Schubert FR, Fainsod A, Gruenbaum Y, Gruss P. 1995. Expression of the

novel murine homeobox Sax-1 in the developing nervous system. Mech Dev 51:99–114.

Schultz CW, Hashimoto R, Brady RM, Gage FH. 1990. Dopaminergic cells align along radial glia in the developing mesencephalon of the rat. Neuroscience 38:427–436.

Shimamura K, Hartigan DJ, Martinez S, Puelles L, Rubenstein JLR. 1995. Longitudinal organization of the anterior neural plate and neural tube. Development 121:3923–3933.

Simeone AD, Acampora D, Gulisano M, Stornaiuolo A, Boncenelli E. 1992. Nested expression domains for four homeobox genes in developing rostral brain. Nature 358:415–436.

Smeets WJAJ, Reiner A. 1994. Catecholamines in the CNS of vertebrates: current concepts of evolution and functional significance. In: Smeets WJAJ, Reiner A, editors. Phylogeny and development of catecholamine systems in the CNS of vertebrates. Cambridge, UK: Cambridge University Press. p 463–481.

Solberg Y, Silvermann WF, Pollack Y. 1993. Prenatal ontogeny of tyrosine hydroxylase gene expression in the rat ventral mesencephalon. Brain Res 73:91–97.

Specht LA, Pickel VM, Joh TH, Reis DJ. 1981. Light-microscopic immunocytochemical localization of tyrosine hydroxylase in prenatal rat brain. I. Early ontogeny. J Comp Neurol 199:233–253.

Stagaard M, Mollgard K. 1989. The developing neuroepithelium in human embryonic and fetal brain studied with vimentin-immunocytochemistry. Anat Embryol (Berl) 180:17–28.

Stoykova A, Gruss P. 1994. Roles of Pax-genes in developing and adult brain as suggested by expression patterns. J Neurosci 14:1395–1412.

Tamada A, Shirasaki R, Murakami F. 1995. Floor plate chemoattracts crossed axons and chemorepels uncrossed axons in the vertebrate brain. Neuron 14:1083–1093.

Timsit S, Martínez S, Allinquant B, Peyron F, Puelles L, Zalc B. 1995. Oligodendrocytes originate in a restricted zone of the embryonic ventral neural tube defined by DM-20 mRNA expression. J Neurosci 15: 1012–1024.

Tremblay P, Pituello F, Gruss P. 1996. Inhibition of floor plate differentiation by Pax3: evidence from ectopic expression in trangenic mice. Development 122:2555–2567.

Vaage S. 1969. Segmentation of the primitive neural tube in chick embryos: a morphological, histochemical and autoradiographical investigation. Adv Anat Embryol Cell Biol 41:1–88.

Van Domburg PHMF, ten Donkelaar HJ. 1991. The human substantia nigra and ventral tegmental area. Adv Anat Embryol Cell Biol 121:1–131.

Van Hartesveldt C, Moore B, Hartman BK. 1986. Transient midline raphe glial structure in the developing rat. J Comp Neurol 253:175–184.

Verney C, Zecevic N, Nikovic B, Alvarez C, Berger B. 1991. Early evidence of catecholaminergic cell groups in 5- and 6-old human embryos using tyrosine-hydroxylase immunocytochemistry. Neurosci Lett 131:121–124.

Verney C, Zecevic N, Gaspar P, Berger B. 1992. Expression of calbindin (CaBP) in human mesencephalic dopaminergic cells (A8-A9-A10) from the 4th embryonic week on: immunocytochemistry of tyrosine hydroxylase and calbindine. Amsterdam: 7th International Catecholamine symposium.

Verney C, Milosevic A, Alvarez C, Berger B. 1993. Immunocytochemical evidence of well-developed dopaminergic and noradrenergic innervations in the frontal cerebral cortex of human fetuses at midgestation. J Comp Neurol 336:331–344.

Verney C, Zecevic N, Ezan P. 2000. Expression of calbindin D28K in the dopaminergic mesotelencephalic system in embryonic and fetal human brain. J Comp Neurol 429:45–58.

Vigny A, Henry JP. 1981. Bovine adrenal tyrosine hydroxylase: comparative study of native and proteolysed enzyme and their interaction with anions. J Neurochem 36:483–489.

Voorn P, Kalsbeek A, Jorritsma-Byham B, Groenewegen HJ. 1988. The pre- and postnatal development of the dopaminergic cell groups in the ventral mesencephalon and the dopaminergic innervation of the striatum of the rat. Neuroscience 25:857–887.

Wallace JA, Lauder JM. 1983. Development of the serotoninergic system in the rat embryo: an immunocytochemical study. Brain Res Bull 10:459–479.

Wang MZ, Jin P, Bumcrot DA, Marigo V, Mc Mahon AP, Wang EA, Woolf T, Pang K. 1995. Induction of dopaminergic neuron phenotype in the midbrain by sonic hedgehog protein. Nat Med 1:1184–1188.

Yamada T, Pfaff SL, Edlund T, Jessell TM. 1993. Control of cell pattern in the neural tube: motor neuron induction by diffusible factors from notochord and floor plate. Cell 73:673–686.

Zecevic N, Verney C. 1995. Development of the catecholamine neurons in human embryos and fetuses, with special emphasis on the innervation of the cerebral cortex. J Comp Neurol 351:509–535.

Zetterström RH, Solomin L, Jansson L, Hoffer BJ, Olson L, Perlmann T. 1997. Dopamine neuron agenesis in Nurr-1-deficient mice. Science 276:248–250.